

**CROSS CALIBRATION OF BONE MINERAL DENSITY VALUES
AMONG THREE DUAL ENERGY X-RAY ABSORPTIOMETRY
SYSTEMS**

The image features a large, faint watermark of the Mahidol University logo in the background. The logo is circular and contains a central emblem with a crown and two lions. The Thai text 'มหาวิทยาลัยมหิดล' (Mahidol University) is written around the perimeter of the circle.

SASITHORN AMNUAYWATTAKORN

**A THESIS SUBMITTED IN PARTIAL FULFILLMENT
OF THE REQUIREMENTS FOR
THE DEGREE OF MASTER OF SCIENCE
(MEDICAL PHYSICS)
FACULTY OF GRADUATE STUDIES
MAHIDOL UNIVERSITY
2011**

COPYRIGHT OF MAHIDOL UNIVERSITY

Copyright by Mahidol University

Thesis
entitled
**CROSS CALIBRATION OF BONE MINERAL DENSITY VALUES
AMONG THREE DUAL ENERGY X-RAY ABSORPTIOMETRY
SYSTEMS**

.....SASITHORN AMNUAYWATTAKORN
.....

Miss Sasithorn Amnuaywattakorn
Candidate

C. Sritara
.....

Asst. Prof. Chanika Sritara, M.D.
M.Sc. (Nuclear Medicine)
M.Sc. (Clinical Epidemiology)
Major advisor

Kan Tham
.....

Mrs. Kanungnij Thamnirat, M.D.
(Thaiboard of Nuclear Medicine)
Co-advisor

B. Mahai
.....

Prof. Banchong Mahaisavariya,
M.D., Dip. Thai Board of Orthopedics
Dean
Faculty of Graduate Studies
Mahidol University

Puangpen Tangboonduangjit
.....

Lect. Puangpen Tangboonduangjit,
Ph.D. (Medical Radiation Physics)
Program Director
Master of Science Program
in Medical Physics
Faculty of Medicine
Ramathibodi Hospital
Mahidol University

Thesis
entitled
**CROSS CALIBRATION OF BONE MINERAL DENSITY VALUES
AMONG THREE DUAL ENERGY X-RAY ABSORPTIOMETRY
SYSTEMS**

was submitted to the Faculty of Graduate Studies, Mahidol University
for the degree of Master of Science (Medical Physics)

on
August 18, 2011

SASITHORN AMNUAYWATTAKORN
.....
Miss Sasithorn Amnuaywattakorn
Candidate

S. Panichkul
.....
Asst. Prof. Suthee Panichkul, M.D.
M.Sc. (Clinical Epidemiology)
Member

Chiraporn Tocharoenchai
.....
Assoc. Prof. Chiraporn Tocharoenchai,
Ph.D. (Biomedical Engineering)
Chair

K. Th
.....
Mrs. Kanungnij Thamnirat, M.D.
(Thaiboard of Nuclear Medicine)
Member

C. Sritara
.....
Asst. Prof. Chanika Sritara, M.D.
M.Sc. (Nuclear Medicine)
M.Sc. (Clinical Epidemiology)
Member

B. Mahaisavariya
.....
Prof. Banchong Mahaisavariya,
M.D., Dip. Thai Board of Orthopedics
Dean
Faculty of Graduate Studies
Mahidol University

Rajata Rajatanavin
.....
Prof. Rajata Rajatanavin
M.D., F.A.C.E.
Dean, Faculty of Medicine
Ramathibodi Hospital
Mahidol University

ACKNOWLEDGEMENTS

I would like to acknowledge to all those who gave me the possibility to complete this thesis.

I would like to express my sincere gratitude and deep appreciation to Assistant Professor Chanika Sritara (M.D.) my advisor for her guidance, supervision and encouragement. I would like to thank my co-advisor, Kanungnij Thamnirat(M.D.) for her valuable suggestion.

I would like to thank Associate Professor Chiraporn Tocharoenchai for her valuable suggestion and comments.

I would like to thank Assistant Professor Sawwanee Asavaphatiboon for her valuable suggestion.

I would like to thank Miss Sasivimol Promma and Miss Suchawadee Musikarat, my sisters, best friends and co-workers, for their kindness in support, comments and understanding with love and care.

I would like to thanks to my co- workers at the division of Nuclear Medicine at Ramathibodi hospital.

I would like to thank Lect. Puangpen Tangboonduangjit, Chair of Science program in Medical Physics, Faculty of Medicine, Ramathibodi Hospital and the lectures of Medical Physics program for their valuable advice.

Finally, I owe unending gratitude to my dear parents and my family for their love, encouragement, and understanding, support and other help throughout my study.

Sasithorn Amnuaywattakorn

CROSS CALIBRATION OF BONE MINERAL DENSITY VALUES AMONG THREE DUAL ENERGY X-RAY ABSORPTIOMETRY SYSTEMS

SASITHORN AMNUAYWATTAKORN 5036370 RAMP/M

M.Sc. (MEDICAL PHYSICS)

THESIS ADVISORY COMMITTEE: CHANIKA SRITARA, M.D., M.Sc.
(NUCLEAR MEDICINE), M.Sc. (CLINICAL EPIDEMIOLOGY),
KANUNGNIJ THAMNIRAT, M.D., THAIBOARD OF NUCLEAR MEDICINE.

ABSTRACT

The generalized Least Significant Change (GLSC) is at a 95% confidence interval of precision error in the bone mineral density (BMD). The objectives of the research were to generate the GLSC values among three DXA machines (Lunar Model Prodigy, HOLOGIC Model Discovery A and Discovery W), to predict Bone mineral Density (BMD) values from cross calibration equations, and to compare our predicted BMDs. Our research – derived with equations together with those from the manufacturers equations and observed BMDs from actual measurements. BMD measurements were performed on 30 females (age 20-80 years) at the lumbar spine and proximal femur. Each site was measured with all 3 DXA machines twice with repositioning in between. All measurement and analysis steps complied with the ISCD official position. The GLSCs were as follows: between Lunar Prodigy and Hologic Discovery A at the lumbar spine, the neck of femur and the total hip is at 0.066, 0.088, and 0.066 (g/cm^2), respectively; between Lunar Prodigy and Hologic Discovery W at the lumbar spine, the neck of femur and the total hip is at 0.064, 0.076, and 0.070 (g/cm^2), respectively; between Hologic Discovery A and Hologic Discovery W at the lumbar spine, the neck of femur and the total hip is at 0.020, 0.074, and 0.062 (g/cm^2), respectively. The comparison of the errors from both equations found that the lumbar spine and total hip were statistically significant but not statistically significant at the neck of femur. These errors were larger than GLSCs therefore, the calculation of GLSCs by using the data collection was more appropriate for cross-calibration of the BMDs than the calculated BMDs from both equations.

KEY WORDS: CROSS CALIBRATION / DXA/BMD

86 pages

การเปรียบเทียบค่าความหนาแน่นของกระดูกระหว่างเครื่องวัดความหนาแน่นของกระดูกโดยใช้เอกซเรย์ 2 ค่าพลังงาน 3 เครื่อง

CROSS CALIBRATION OF BONE MINERAL DENSITY VALUES AMONG THREE DUAL ENERGY X-RAY ABSORPTIOMETRY SYSTEMS

ศศิธร อำนวยวิทย์ 5036370 RAMP/M

วท.ม. (ฟิสิกส์การแพทย์)

คณะกรรมการที่ปรึกษาวิทยานิพนธ์ : ชนิกา ศรีธรา, พ.ม., วท.ม., คณิงนิจ ธรรมรัตน์, พ.ม.

บทคัดย่อ

Generalized least significant change (GLSC) เป็นค่าช่วงเชื่อมั่นร้อยละ 95 ของค่า Precision Error ในการวัดความหนาแน่นกระดูก (Bone mineral density, BMD) วัดดูประสงค์ของการวิจัยนี้เพื่อหาค่า GLSC จาก DXA 3 เครื่อง (Lunar รุ่น Prodigy และ Hologic รุ่น Discovery A, Discovery W) และทำนายค่า BMD จากสมการ cross calibration ของผู้วิจัยรวมถึงเปรียบเทียบค่า BMD ที่ได้จากงานวิจัยและค่า BMD ที่ได้จากสมการ cross calibration ของผู้ผลิตกับค่า BMD ที่วัดได้จริง มีผู้ลงนามเข้าร่วมการวิจัย 30 ราย (เพศหญิง ช่วงอายุ 20-80 ปี) รับการตรวจวัดค่า BMD ในส่วนของ Lumbar spine และ Proximal femur ทำการตรวจส่วนละ 2 ครั้งด้วยเครื่อง DXA ทั้ง 3 เครื่องโดยมีการจัดทำ และวิเคราะห์ผลตามมาตรฐาน ISCD ค่า GLSC ระหว่าง Lunar Prodigy กับ Hologic Discovery A บริเวณ Lumbar spine, Neck of femur และ Total hip เท่ากับ 0.066, 0.088 และ 0.066 (g/cm^2) ตามลำดับ, ระหว่าง Lunar Prodigy กับ Hologic Discovery W บริเวณ Lumbar spine, Neck of femur และ Total hip เท่ากับ 0.064, 0.076 และ 0.070 (g/cm^2) ตามลำดับ และ ระหว่าง Hologic Discovery A กับ Hologic Discovery W บริเวณ Lumbar spine, Neck of femur และ Total hip เท่ากับ 0.020, 0.074 และ 0.062 (g/cm^2) ตามลำดับ เมื่อเปรียบเทียบค่าความผิดพลาดของสมการจากทั้ง 2 แหล่ง พบว่ามีความแตกต่างอย่างมีนัยสำคัญทางสถิติที่ Lumbar spine และ Total hip และไม่มีนัยสำคัญที่ Neck of femur ค่าความผิดพลาดนี้มีขนาดใหญ่กว่าค่า GLSC ดังนั้นในการเปรียบเทียบควรทำการเก็บข้อมูลเพื่อคำนวณหาค่า GLSC มากกว่าการประมาณค่า BMD ของการตรวจครั้งก่อนหน้าด้วยการคำนวณจากสมการ ไม่ว่าจะสมการนั้นจะเป็นสมการที่หาโดยแต่ละสถาบันหรือจากบริษัทผู้ผลิต

CONTENTS

	Page
ACKNOWLEDGEMENTS	iii
ABSTRACT (ENGLISH)	iv
ABSTRACT (THAI)	v
LIST OF TABLES	vii
LIST OF FIGURES	viii
LIST OF ABBREVIATIONS	xi
CHAPTER I INTRODUCTION	1
CHAPTER II OBJECTIVES	7
CHAPTER III LITERATURE REVIEW	8
CHAPTER IV MATERIALS AND METHODS	42
CHAPTER V RESULTS	57
CHAPTER VI DISCUSSION AND CONCLUSION	71
REFERENCES	74
APPENDICES	76
BIOGRAPHY	86

LIST OF TABLES

Table	Page
3.1 Component and function of DXA	16
3.2 Filters and their resulting X-ray peaks from different DXA manufacturer	18
4.1 Machine in system 1 and system 2	55
5.1 Volunteer's characteristics	57
5.2 GLSC from system 1 to system 2	57
5.3 Cross calibration equation between Lunar Prodigy and Hologic Discovery A	58
5.4 Cross calibration equation between Lunar Prodigy and Hologic Discovery W	58
5.5 Cross calibration equation between Hologic Discovery A and Hologic Discovery W	58
5.6 95% confidence interval of difference between observed and predicted BMD using research equations and manufacturer equations (cross calibration equations between Lunar Prodigy and Hologic Discovery A)	59
5.7 95% confidence interval of difference between observed and predicted BMD using research equations and manufacturer equations (cross calibration equations between Lunar Prodigy and Hologic Discovery W)	63
5.8 95% confidence interval of difference between observed and predicted BMD using research equations and manufacturer equations (cross calibration equations between Hologic Discovery A and Hologic Discovery W)	67

LIST OF FIGURES

Figure	Page
3.1 Structure of cortical and trabecular bone	8
3.2 Bone remodeling	12
3.3 X-ray spectra for Switched kV techniques	17
3.4 Relationship of relative intensity and photon energy before filtering	19
3.5 Relationship of relative intensity and photon energy after filtering with cerium	19
3.6 Relationship of relative intensity and photon energy in Switching and Filtering methods	20
3.7 Wheel or Drum	22
3.8 Calibration Block (Lunar Prodigy)	23
3.9 Hip's regions of interest for Hologic	24
3.10 Hip's regions of interest for Lunar	25
3.11 AP lumbar spine positioning	28
3.12 Laser light position in AP lumbar spine	29
3.13 AP lumbar spine analysis (Lunar Prodigy)	30
3.14 AP Lumbar spine analysis (Hologic Discovery)	30
3.15 Proximal femur positioning	32
3.16 Laser light position in proximal femur	32
3.17 Proximal femur analysis (Lunar Prodigy)	33
3.18 Proximal femur analysis (Hologic Discovery)	33
3.19 Result of cross-calibration between Hologic Delphi and Lunar Prodigy	39
3.20 Relationship between number of sample size and magnitude of GLSC	41

LIST OF FIGURES (cont.)

Figure	Page
4.1 Hologic Discovery and Console	46
4.2 Spine phantom	46
4.3 Position of Hologic spine phantom	47
4.4 ROI of spine phantom in the daily Q.C.	48
4.5 Hologic Discovery daily Q.C. data Plot	49
4.6 Lunar Prodigy	50
4.7 Calibration Block	50
4.8 Aluminum Spine Phantom	50
4.9 Position of Calibration Block in the daily Q.C	51
4.10 Result of daily Q.C.	52
4.11 Laser and spine phantom in daily Q.C. Lunar Prodigy	53
4.12 Lunar Prodigy Daily Q.C. data	53
5.1 Plot of mean and difference Altman and Bland between research's cross calibration equations vs. manufacturer's cross calibration equations in Lunar Prodigy and Hologic Discovery A at the lumbar spine	60
5.2 Plot of mean and difference Altman and Bland between research's cross calibration equations vs. manufacturer's cross calibration equations in Lunar Prodigy and Hologic Discovery A at the neck of femur	61
5.3 Plot of mean and difference Altman and Bland between research's cross calibration equations vs. manufacturer's cross calibration equations in Lunar Prodigy and Hologic Discovery A at the total hip	62

LIST OF FIGURES (cont.)

Figure	Page
5.4	64
Plot of mean and difference Altman and Bland between research's cross calibration equations vs. manufacturer's cross calibration equations in Lunar Prodigy and Hologic Discovery W at the lumbar spine	
5.5	65
Plot of mean and difference Altman and Bland between research's cross calibration equations vs. manufacturer's cross calibration equations in Lunar Prodigy and Hologic Discovery W at the neck of femur	
5.6	66
Plot of mean and difference Altman and Bland between research's cross calibration equations vs. manufacturer's cross calibration equations in Lunar Prodigy and Hologic Discovery W at the total hip	
5.7	68
Plot of mean and difference Altman and Bland between research's cross calibration equations vs. manufacturer's cross calibration equations in Hologic Discovery A and Hologic Discovery W at the lumbar spine	
5.8	69
Plot of mean and difference Altman and Bland between research's cross calibration equations vs. manufacturer's cross calibration equations in Hologic Discovery A and Hologic Discovery W at the neck of femur	
5.9	70
Plot of mean and difference Altman and Bland between research's cross calibration equations vs. manufacturer's cross calibration equations in Hologic Discovery A and Hologic Discovery W at the total hip	
D	86
Questionnaires	

LIST OF ABBRAVIATIONS

Abbreviations	Term
BMC	Bone mineral content
BMD	Bone mineral density
BMU	Bone remodeling unit
CBDT	Certified Bone Densitometry Technologists
CCD	Certified Clinical Densitometrists
CdWO ₄	Cadmium Tungstate
CV	Coefficient of variation
CZT	Cadmium zinc telluride
DXA	Dual energy x-ray absorptiometry
Eq	Equation
GLSC	Generalized Least Significant Change
ILSC	Ideal Least Significant Change
ISCD	The International Society for Clinical Densitometry
keV	Kilo electron volt
LSC	Least significant change
PDC	Position Development Conference
PMT	Photomultiplier tube
QC	Quality Control
ROI	Region of interest
RMS	Root Mean Square
SD	Standard deviation
WHO	World Health Organization

CHAPTER I

INTRODUCTION

Osteoporotic fractures have come to be recognized as one of the most serious problems in public health. For a 50-y-old white woman, the lifetime risk of suffering a fragility fracture of the spine, hip, or forearm is estimated to be 30%–40%, which compares with the percentages for breast cancer and cardiovascular disease of 9%–12% and 30%–40%, respectively. For men, the risk of an osteoporotic fracture is about one third of that in women. In the United States in 1995, the total health care costs attributable to osteoporotic fractures exceeded \$13 billion, a figure that is expected to rise to between \$30 and \$40 billion by the year 2020. (1)

The post - menopause clinic of Chulalongkorn Hospital in Thailand studied the prevalence of osteoporosis in 1,047 patients, age ranged from 41 to 60 years. The results showed that the prevalence of osteoporosis in women that post - menopause was 11.9% and 21.4% for femoral neck and L-spine, respectively. (2, 3)

In 1999, there was collaboration of Chulalongkorn University, Red Cross, Ministry of public health, and WHO. The population of Thailand that was 40 years up women was chosen at random. The result shows the prevalence of osteoporosis is 13.6% and 19.75% for femoral neck and L-spine, respectively. (2, 4)

Hip fracture was the most cause of the death and two thirds of hip fracture patient was died within 1 year after bone fracture. In addition to incurring greater costs, hip fractures also cause greater morbidity and mortality than other types of fractures. One quarter of hip-fracture patients die within a year after their fracture, and survivors frequently suffer sustained disability and loss of independence. However, it should not be forgotten that fractures at other sites may also cause substantial pain and disability. The increased recognition of the scale of morbidity and mortality attributable to osteoporosis has led to a major effort by the pharmaceutical industry to develop new therapeutic strategies for the prevention of fractures. Estrogen deficiency after menopause is one of the most documented causes of osteoporosis and can be

prevented by hormone replacement therapy (HRT). However, although HRT has additional benefits that include the prevention of cardiovascular disease, it may also cause an increase, of approximately 35%, in the risk of breast cancer in long-term users. In addition to such fears, compliance with HRT may also be a problem because of side effects such as bleeding, weight gain, and breast tenderness. Consequently, much effort has been devoted to developing alternative treatments for osteoporosis. Among these treatments, bisphosphonates are becoming increasingly recognized as the treatment of choice at the present time. Another new class of therapeutic agents recently introduced is the selective estrogen receptor modulators (SERMs), which are compounds that have a unique ability to mimic the beneficial effects of HRT on osteoporosis and cardiovascular disease while antagonizing the effects of estrogen on the breast and uterus. (1)

The osteoporosis is the main problem of public health in Thailand. The Bone Mineral Density (BMD) was used for diagnosis and follow up in this disease. Especially, the osteoporosis was recommended to check less than 1 time per year. For analysis, the BMD value of patient was compared with previous value. Thus, the accuracy and precision (reproducibility) of this value should be considered.

The change of BMD occurs when the BMD value differ more than 95 % Confidence Interval (CI) of precision error that this value is Generalized Least Significant Change (GLSC). For indication of the treatment efficiency, the factor that involve with BMD value was controlled with same parameter in previous check. Furthermore, measurement and calculation techniques of each model and manufacturer are difference. Due to method of generate dual energy x-ray, type of detector, calibration tool and technique, and analysis algorithms. Those factors affect to an intensity of radiation to irradiate patient, a different count value and an equation for calculation. Thus, the comparison of the BMD value with different model and manufacture was tested with patient. (4)

The factors that affect the BMD value in dual energy x-ray absorptiometry (DXA) (5) are as follows;

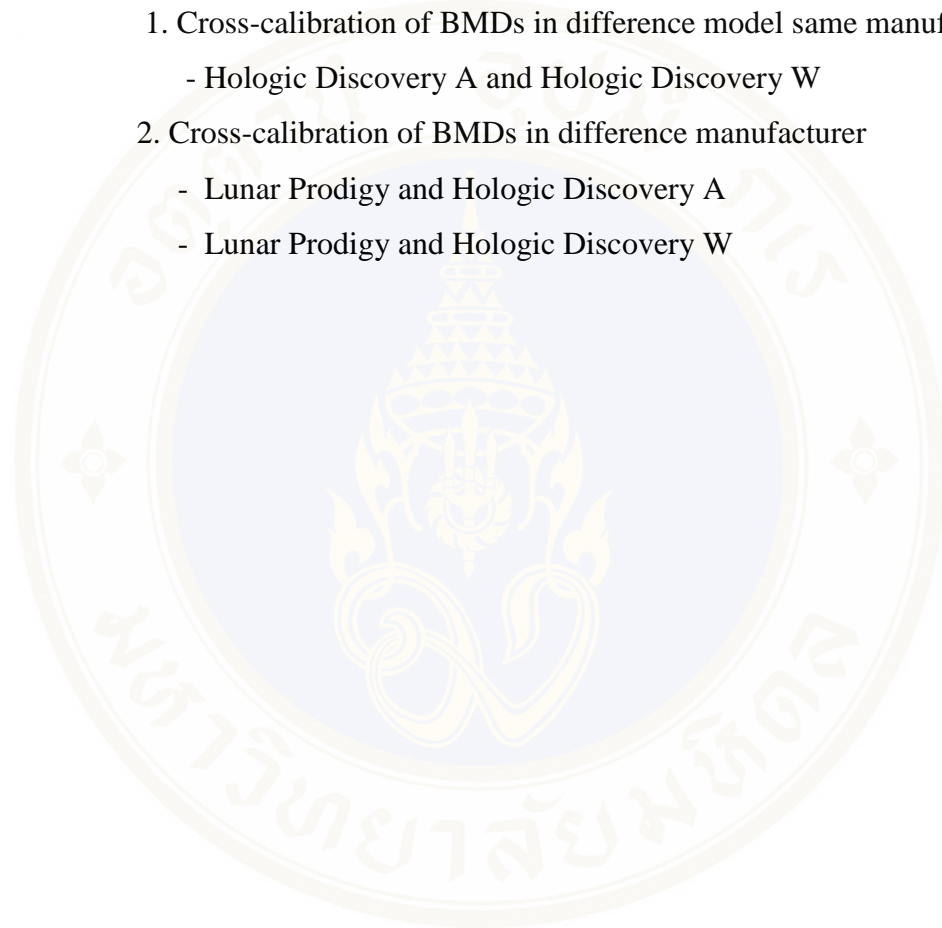
1. Dual energy x-ray absorptiometry (DXA)
 - 1.1 Methods of generate dual energy x-ray
 - 1.2 Detector type
 - 1.3 Edge detection software
 - 1.4 Calibration technique
 - 1.5 Region Of Interest (ROI)
2. Technologist Precision
 - 2.1 Patient positioning and analysis

Due to there are a lot of factors to the BMDs. Thus, the precision error should be analyzed. And the comparison of the BMDs between machines can be done when Generalized Least Significant Change (GLSC) value was calculated. The GLSCs of the both machines must be more than the GLSCs with same machine.

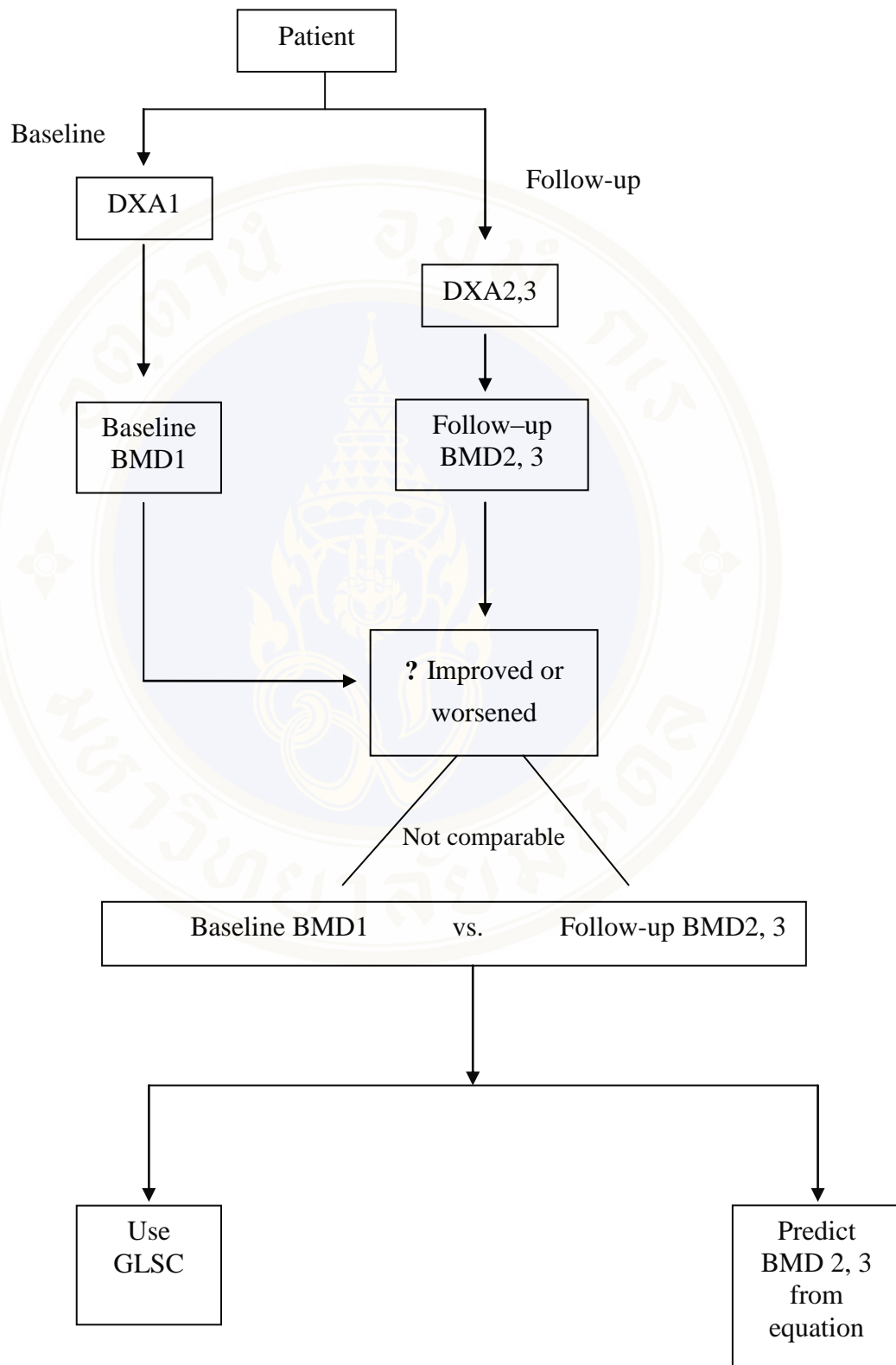
The main purpose of this study is to generate the GLSC value of three DXA machines at division of Nuclear Medicine, Ramathibodi Hospital, to diagnosis the change of BMD from the measurement. We have presented an equation to calculate the GLSC between 2 measures on 3 different DXA systems. If the magnitude of the difference between a patient's baseline BMD measured on system 1 and their follow up BMD measured on system 2 is greater than the GLSC, then there is 95% confidence interval that a true change in BMDs has occurred and if the difference between a patient's baseline BMD measure on system 1 and their follow up BMD measure on system 2 is lesser than the GLSC, then there is 95% confidence interval that a variation of measure occurred.

DXA systems at division of Nuclear Medicine, Ramathibodi Hospital were replaced into the different model and difference manufacturer which caused the comparison problem between the previous BMDs and the present or follow up BMDs. Then the cross-calibrations of BMDs from the different machines were useful. In this study, the cross-calibration of BMDs of then different systems was evaluated.

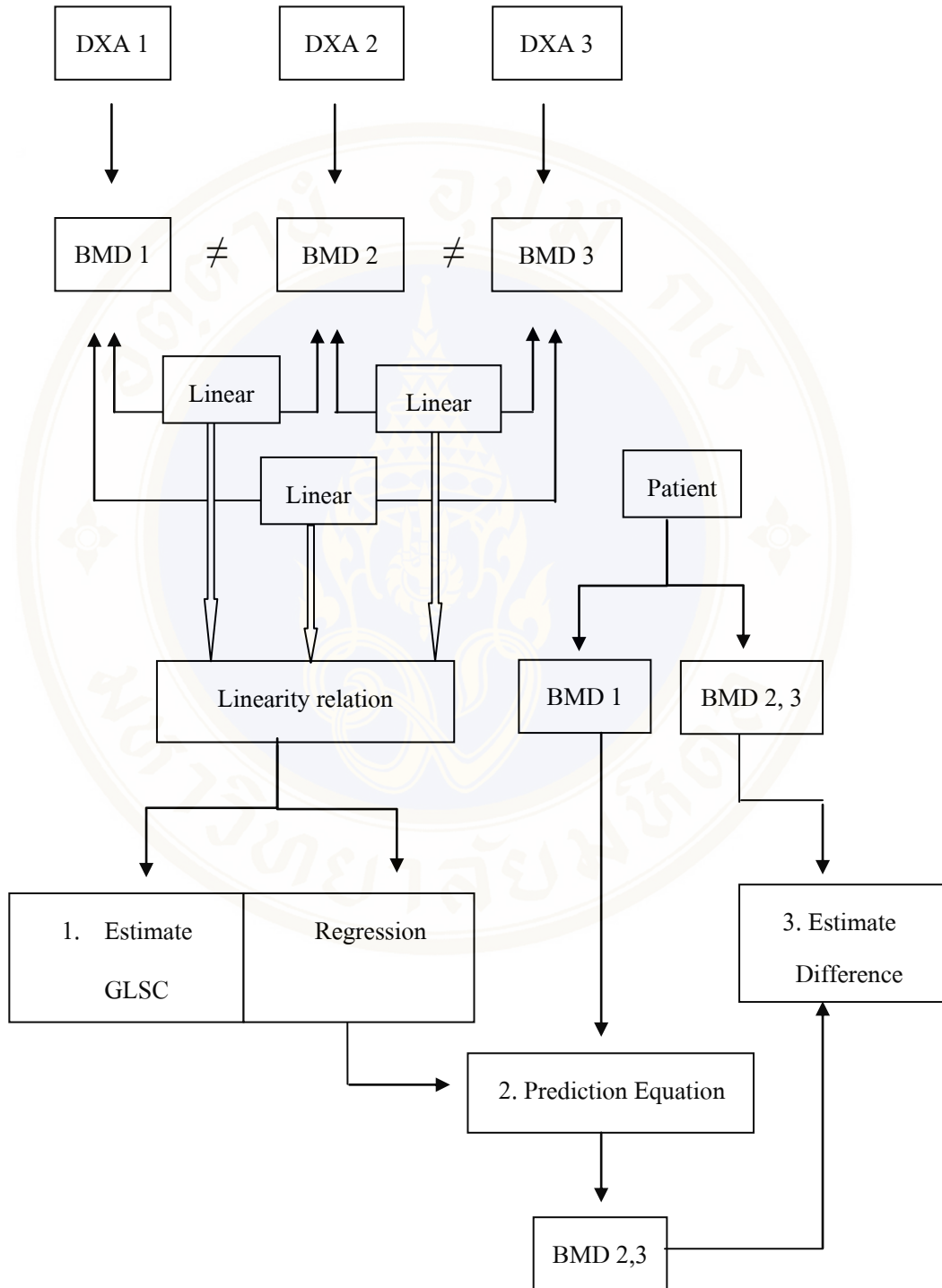
1. Cross-calibration of BMDs in difference model same manufacturer
 - Hologic Discovery A and Hologic Discovery W
2. Cross-calibration of BMDs in difference manufacturer
 - Lunar Prodigy and Hologic Discovery A
 - Lunar Prodigy and Hologic Discovery W



Conceptual Framework 1



Conceptual Framework 2



CHAPTER II

OBJECTIVES

The objectives of this study are:

- 2.1 To estimate Generalized Least Significant Change (GLSC) of Dual Energy X-ray Absorptiometry (DXA) from Lunar Prodigy, Hologic Discovery A and Discovery W at Division of Nuclear Medicine at Ramathibodi Hospital.
- 2.2 To predicted cross calibration equation from Lunar Prodigy, Hologic Discovery A and Discovery W.
- 2.3 To study the compare predicted BMDs between research's cross calibration equation and manufacturer's cross calibration equation.

CHAPTER III

LITERATURE REVIEW

3.1 Bone(6-8)

The strength and stiffness of bone give vertebrates mobility, dexterity, and strength. Bone is classified into three shapes: long bones, short bones, and flat bones. Bone tissue assumes two forms: outer cortical or compact bone and inner cancellous or trabecular bone. These forms are demonstrated (Fig. 3.1). Cortical bone forms about 80% of the skeleton and surrounds thin plates of cancellous bone with compact lamellae. Cortical and cancellous bones modify their structure in response to changes in loading, hormonal influences, and other factors. Cortical bone has greater density and has compressive strength greater than that of cancellous bone due to the fact that the compression strength of bone is proportional to the square of the density.

Compact Bone & Spongy (Cancellous Bone)

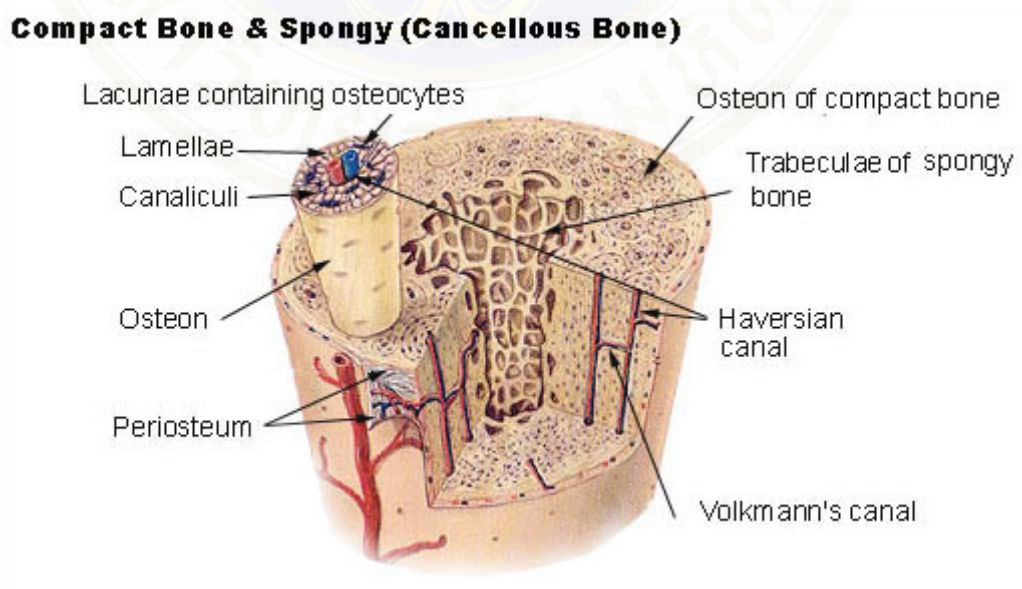


Figure 3.1 Structure of cortical and trabecular bone (8)

For microscopic structure, osteoblasts form unmineralized bone organic matrix, called osteoid, on the surface of mineralized bone matrix during skeletal growth and bone remodeling (Fig. 3.2). Osteoid normally mineralizes soon after it appears so normal bone contains only small amounts of unmineralized matrix. Osteoid lacks the stiffness of mineralized bone matrix. Therefore, failure to mineralize bone matrix during growth or during normal turnover in mature individuals produces weaker bone. Individuals with impaired mineralization of bone matrix may develop skeletal deformities in children or fractures in adults.

Mineralized bone consists of two forms: woven (immature, fiber, or primary) bone and lamellar (mature, secondary) bone. Woven bone forms the embryonic skeleton and new bone in the metaphyseal parts of growth plates. During skeletal growth and as the skeleton develops, mature bone replaces the woven bone. Woven bone is the first bone formed in healing fractures and during rapid turnover and formation of bone associated with metabolic, neoplastic, and infectious or inflammatory diseases. Cells rapidly form irregular, almost random, collagen fibril matrix of woven bone giving woven bone its name. Woven bone contains approximately four times as many osteocytes per unit volume of lamellar bone, and they vary in size, orientation, and distribution. Mineralization of woven bone follows an irregular pattern with mineral deposits varying in size and relationship to collagen fibrils. Lamellar bone is formed more slowly and the cell density is less. Collagen fibrils of lamellar bone vary less in diameter and lie in tightly aligned parallel sheets forming lamellae 4 to 12 microns thick in a uniform distribution of mineral throughout the matrix. Woven bone lacks collagen fibril orientation, has high cell and water content and irregular mineralization making woven bone more flexible, more easily deformed, and weaker than mature lamellar bone. Therefore, immature skeleton and healing fractures have less stiffness and strength than mature skeleton or a fracture remodeled with lamellar bone.

Bone cells are separated into four groups depending on their morphology, function, and characteristics: undifferentiated or osteoprogenitor cells, osteoblasts, osteocytes, and osteoclasts.

Undifferentiated or osteoprogenitor cell are small cells with single nuclei, few organelles, and irregular forms which remain in an undifferentiated state until

stimulated to proliferate or differentiate into osteoblasts. They reside in the canals of bone, endosteum, and periosteum.

Osteoblasts are cuboidal cells with a single eccentric nucleus and contain a large amount of synthetic organelles, such as endoplasmic reticulum and Golgi membranes. They lie on bone surfaces and form new bone matrix and participate in controlling matrix mineralization. When active, they become round, oval or polyhedral in form and new osteoid separates them from mineralized matrix. Cytoplasmic processes extend through the osteoid to contact osteocytes within the mineralized matrix. When synthesizing new matrix, they can either decrease synthetic activity, remain on the bone surface, and become the flatter form of a bone surface lining cell or they can surround themselves with matrix and become osteocytes.

Osteocytes when combined with periosteal and endosteal cells cover bone matrix surfaces. They contribute more than 90% of the cells of the mature skeleton, and their cell membranes and cell processes cover more than 90% of the total surface area of mature bone matrix. Long cytoplasmic processes extend from their oval- or lens-shaped bodies to contact other osteocytes or cell processes of osteoblasts, forming a network of cells that extends from the bone surfaces throughout the bone matrix. Osteocytes have access to almost all the mineralized matrix surface area and they may have an important role in the cell mediated exchange of mineral that occurs between bone fluid and blood. They help maintain the composition of bone fluid and the body's mineral balance.

Osteoclasts are large irregular cells with multiple nuclei. Their cytoplasm is filled with mitochondria to supply energy to resorb bone. Osteoclasts lie directly against the bone matrix on endosteal, periosteal, and Haversian system bone surfaces, but they can move from one site of bone resorption to another. They form by fusion of multiple bone marrow-derived mononuclear cells. When they finish bone resorption, they may divide to reform multiple mononuclear cells. They have complex folding of their cytoplasmic membrane at sites of bone resorption. This border plays a critical role in bone resorption, possibly by increasing the surface area of the cell relative to bone and creating a localized environment that rapidly degrades bone matrix. The fluid between this brush border and bone matrix may have a high concentration of hydrogen ions and proteolytic enzymes where the acidic environment can

demineralize bone matrix, and the enzymes can degrade organic bone matrix. In cancellous bone, osteoclasts resorb bone surface creating a depression called a Howship's lacuna. In cortical bone, osteoclasts lead the osteonal cutting cones that remodel dense cortical bone.

Bone matrix consists of organic macromolecules, inorganic mineral, and matrix fluid. Inorganic matrix contributes approximately 70 to 80% of wet bone weight, organic macromolecules contribute about 20% of wet bone weight, and water contributes about 8 to 10%. Organic matrix gives bone its form and provides tensile strength, while mineral component give bone strength during compression. Removal of either organic or inorganic component leaves bone in its original form and shape. Demineralized bone, like tendon or ligament, has great flexibility. Removal of organic matrix makes bone brittle. A slight deformation will crack the inorganic matrix and a sharp blow will shatter it.

Bony organic matrix resembles dense fibrous tissues like tendon, ligament, and joint capsule. Type I collagen contributes over 90% of the organic matrix, while 10 % is comprised of small proteoglycans, many non-collagenous proteins including osteonectin and small amounts of type V collagen and other collagens. Mineralization changes and stabilizes the composition of organic matrix. Once mineralization occurs, the organic matrix remains stable until resorbed. Abnormalities of organic matrix can weaken bone.

Soon after osteoblasts produce osteoid, mineral appears within the bone type I collagen fibrils, and then extends through the matrix without altering the organization of collagen fibrils or affecting the osteocytes within the mineralized matrix. Mineralized inorganic bone matrix increases the stiffness and strength of bone and provides a reservoir for minerals needed for normal function of other tissues and organ systems. The bone matrix contains approximately 99% of the body's calcium, 80% of the phosphate, and large amounts of sodium, magnesium, and carbonate. Newly mineralized bone matrix contains a variety of calcium phosphate species that range from relatively soluble complexes to insoluble crystalline hydroxyapatite. As bone matures, the inorganic matrix becomes crystalline hydroxyapatite with some amount of sodium, magnesium, citrate, and fluoride. The degree of mineralization increases with maturation, so the material properties of bone change: with increasing

mineralization, bone stiffness increases. This change explains the different patterns of fracture between adults and children. Normal adult bone usually breaks rather than deforming permanently, whereas, children's bones may bow or buckle rather than break.

Osteoclasts remove bone matrix and osteoblasts replace it. This physiologic turnover seen in Figure 3.2 may have a role in maintaining the structural integrity of bone tissue. To preserve normal bone mass and mechanical properties, osteoblastic bone formation must balance osteoclastic bone resorption. A variety of stimuli can alter this balance. Repetitive loading can increase bone formation, thereby increasing bone mass and strength. Immobilization decreases bone formation, thereby decreasing bone mass and strength. Bone mass normally changes with age. It maximizes at about 10 years after completion of skeletal growth, remains stable for a variable period, then decreases progressively weakening the skeleton. The reasons for bone loss are poorly understood, but bone turnover studies show that both systemic and local factors help control osteoclast and osteoblast function.

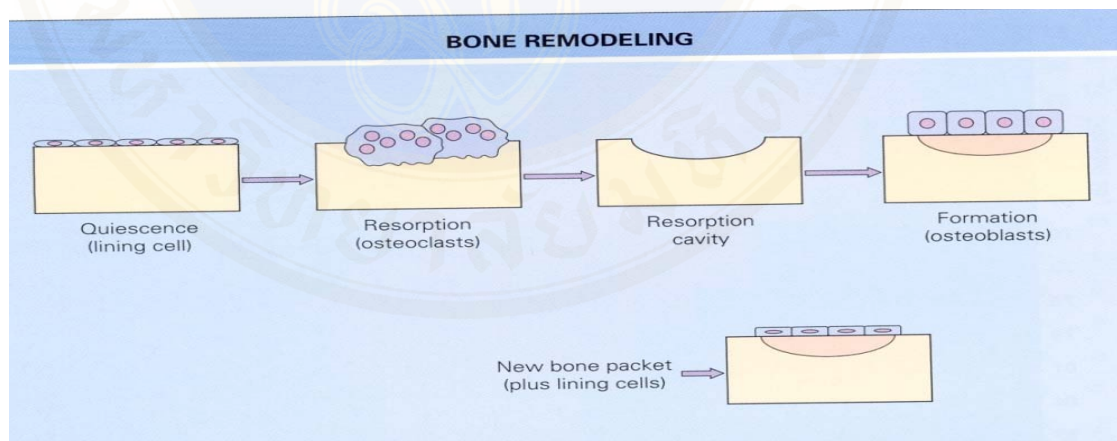


Figure 3.2 Bone remodeling (8)

3.2 Osteoporosis(1)

The term “osteoporosis” is derived from the classical Greek word “osteon” meaning bone, and “poros” meaning a small passage or pore. Thus, the term is descriptive of the changes in bone tissue found in this generalized skeletal disease. The modern definition of osteoporosis is “a systemic skeletal disease characterized by low bone mass and microarchitectural deterioration of bone tissue, with a consequent increase in bone fragility and susceptibility to fracture” It should be noted that this definition does not necessitate that an individual sustain a fracture before a diagnosis of osteoporosis is made but introduces the concept of low bone mass and its relationship to increased fracture risk. Although it could be argued that it is wrong to define a disease on the basis of what is essentially a risk factor (i.e., low bone density), there is nevertheless some logic to this because fractures only occur late in the disease process when skeletal integrity is already severely compromised. Therefore, it is desirable to identify individuals at high risk for osteoporosis, with the goal for beginning treatment early enough to prevent fractures from occurring.

Osteoporotic fractures have come to be recognized as one of the most serious problems in public health. For a 50-y-old white woman, the lifetime risk of suffering a fragility fracture of the spine, hip, or forearm is estimated to be 30%–40%, which compares with the percentages for breast cancer and cardiovascular disease of 9%–12% and 30%–40%, respectively. For men, the risk of an osteoporotic fracture is about one third of that in women. In the United States in 1995, the total health care costs attributable to osteoporotic fractures exceeded \$13 billion, a figure that is expected to rise to between \$30 and \$40 billion by the year 2020. Of these costs, about two thirds are attributable to hip fractures. In addition to incurring greater costs, hip fractures also cause greater morbidity and mortality than other types of fractures. One quarter of hip-fracture patients die within a year after their fracture, and survivors frequently suffer sustained disability and loss of independence.

3.3 WHO classification for osteoporosis (9)

In 1994 a World Health Organization (WHO) recommended a definition of osteoporosis that was based on a Bone Mineral Density (BMD) measurement of the spine and hip expressed in number of standard deviations from the mean (average) value of a young adult population or T-score

$$\text{T-score} = \frac{\text{Measured BMD} - \text{Young adult mean BMD}}{\text{Young adult mean SD}}$$

The World Health Organization (WHO) has set the values for interpreting T-score as:

1. Osteoporosis: T – score equal - 2.5 or less
2. Osteopenia: T – score between – 2.5 to -1
3. Normal: T – score equal -1 or greater

Comparison of patient's current BMD to reference BMD of same age group

$$\text{Z-score} = \frac{\text{Measured BMD} - \text{Age-matched mean BMD}}{\text{Age-matched mean SD}}$$

3.4 Indication for Bone Mineral Density Testing (10)

- Women aged 65 and older.
- Postmenopausal women under age 65 with risk factors for fracture.
- Women during the menopausal transition with clinical risk factors for fracture, such as low body weight, prior fracture, or high-risk medication use.
- Men aged 70 and older.
- Men under age 70 with clinical risk factors for fracture.
- Adults with a fragility fracture.
- Adults with a disease or condition associated with low bone mass or bone loss.
- Adults taking medications associated with low bone mass or bone loss.
- Anyone being considered for pharmacologic therapy.
- Anyone being treated, to monitor treatment effect.
- Anyone not receiving therapy in who evidence of bone loss would lead to treatment.

3.5 Dual Energy X-ray Absorptiometry (DXA)

The component and function of DXA are listed in table 3.1

Table 3.1 Component and function of DXA

Component	Function
3.5.1 X-ray tube - oil –filled metal housing - fixed anode X-ray - lead shielding - collimating devices - filament transformer - electrical connectors	To generate X-ray
3.5.2 High voltage supply	To generate constant potential for X-ray tube
3.5.3 Radiation Detector - Any of the 2 types is used: ▪ CdWO ₄ (Cadmium Tungstate) crystal ▪ CZT (Cadmium zinc telluride) crystal	To receive X-ray from X-ray tube -To receive X-ray and simply pass X-ray to PMT -To receive and change X-ray to electrical current
3.5.4 Photomultiplier tube (Used with only CdWO ₄ crystal)	To change light signals from detector to electrical current
3.5.5 Laser indicator	To mark starting scan position
3.5.6 Preamplifier and Amplifier	To adjust and amplify signal from PMT
3.5.7 Dual channel analyzer	To select optimal signal
3.5.8 Counter	To count signal and send to Analysis part
3.5.9 Data processing device and display	To process and display

3.6 Factors contributing to variation in BMD measurement

3.6.1 Methods for dual energy X-ray generation

Hologic Discovery A and Hologic Discovery W used the X-ray source switching method but Lunar Prodigy used the filtration method.

3.6.1.1 X-ray source switching method

Switching systems switch the high-voltage generator that is connected to the X-ray source, between high or low peak voltages (kVp) during alternate half-cycles of the main power supply. During each cycle, a peak distribution at either 70 keV or 140 keV is produced (Fig. 3.3-3.4). A current-integrating detector system is used. Current-integrating detectors sum all the signal during the half cycle since it is known all of the photons are either high (or low) energy. No need to count and discern the energy. Integrating detector systems do not have limiting upper count rate. However, they are sometimes challenged by low count rates. These systems are continuously calibrated using a rotating wheel or drum (internal calibration).

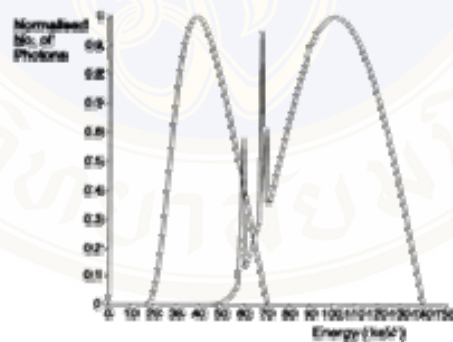


Figure 3.3 X-ray spectra for Switched kV techniques (11)

3.6.1.2 Filtration method

Filtering systems use a constant-potential generator and a K-edge filter to split the polyenergetic X-ray beam into high and low energy components. Table 3.2 shows filters and their resulting X-ray peaks from different DXA manufacturers. Lunar uses a cerium filter that result in energy peak of 38 and 70 keV (Fig. 3.5-3.6). Because either a low or high energy photon can hit the detector at any given moment, the detector needs to determine if the photon was high or low energy. This is done with an energy discriminating detector. The energy discriminating detector counts the high and low energy photons at each image position, a technique called pulse counting. Because it takes time to discriminate and count, photon counting systems have limited count rate capabilities. However, they are very good at measuring low photon counts. For filtering systems an external calibration phantom is often used.

Table 3.2 Filters and their resulting X-ray peaks from different DXA manufacturers

System	X-ray generator(kVp)	Filter	X-ray energy (keV)
LUNAR	76	cerium	38 and 70
NORLAND	100	samarium	46.8 and 80
SOPHA	80	neodymium	43 and 70

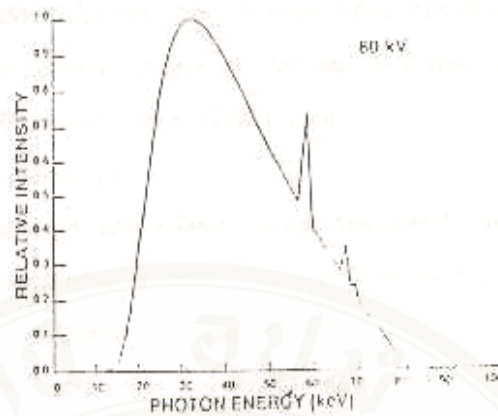


Figure 3.4 Relationship of relative intensity and photon energy before filtering (11)

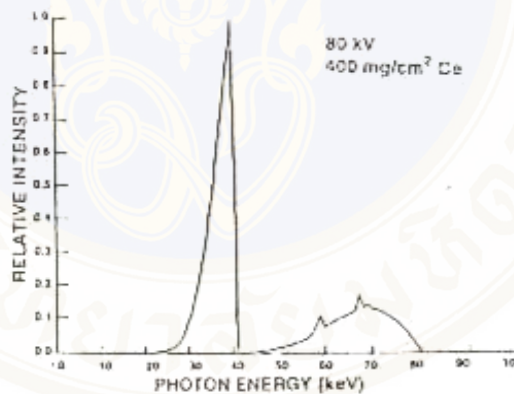


Figure 3.5 Relationship of relative intensity and photon energy after filtering with cerium (11)

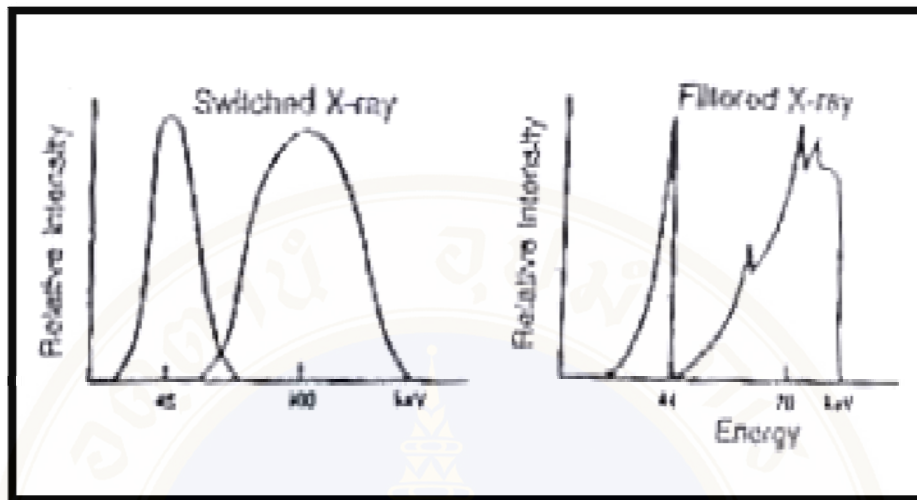


Figure 3.6 Relationship of relative intensity and photon energy in Switching and Filtering methods (11)

3.6.2 Detector (5)

Detector for Hologic uses the Cadmium Tungstate (CdWO_4) detectors perform 2-step conversion by first changing X-ray into light and finally to electronic signals.

Detector for Lunar Prodigy uses the Cadmium zinc telluride (CZT) detectors directly convert X-rays to electronic signals.

3.6.3 Edge detection software (12)

Edge detection for Hologic uses a histogramming approach to separate bone and soft tissue. Newer Hologic machines have “Auto low density” software (that makes assumptions about the anatomy being scanned).

Edge detection for GE Lunar uses a gradient approach. It searches for areas of large attenuation differences across a scan sweep. A rapid change in attenuation (gradient) defines the bone/tissue edge.

3.6.4 Calibration

Hologic Discovery A and Hologic Discovery W used the internal calibration but Lunar Prodigy used the external calibration

3.6.4.1 Internal Calibration

Internal calibration requires oscillating supply. X-ray passes through the calibration filter (Wheel or Drum) while the patient is being scanned. Calibration filter contains 3 types of materials (Fig. 3.7).

1. Air
2. Soft tissue equivalent resin
3. Bone equivalent epoxy

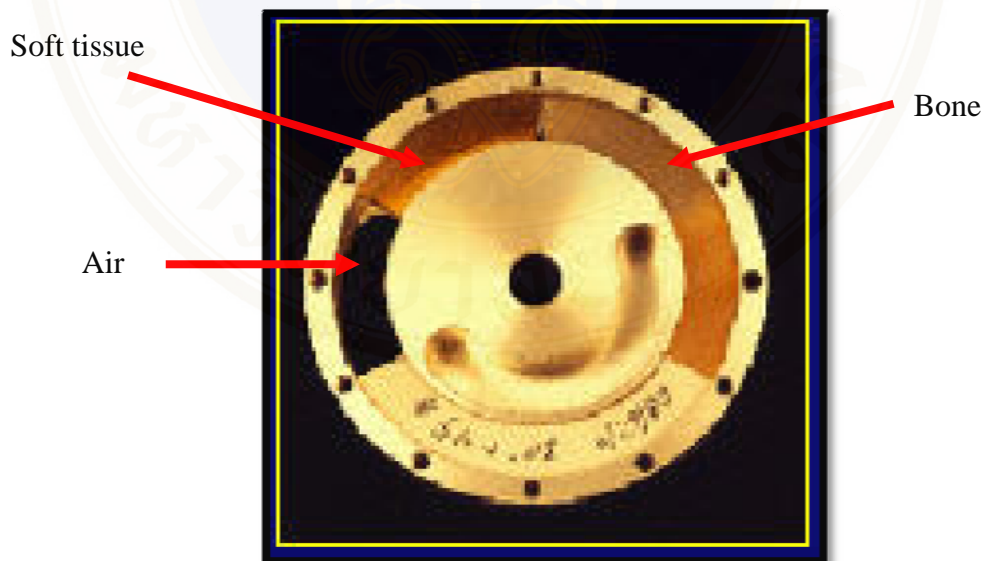


Figure 3.7 Wheel or Drum (11)

3.6.4.2 External device

External calibration uses the calibration block is performed on a daily basis as part of the Quality Control. The calibration block contains bone and tissue standards (Fig. 3.8).

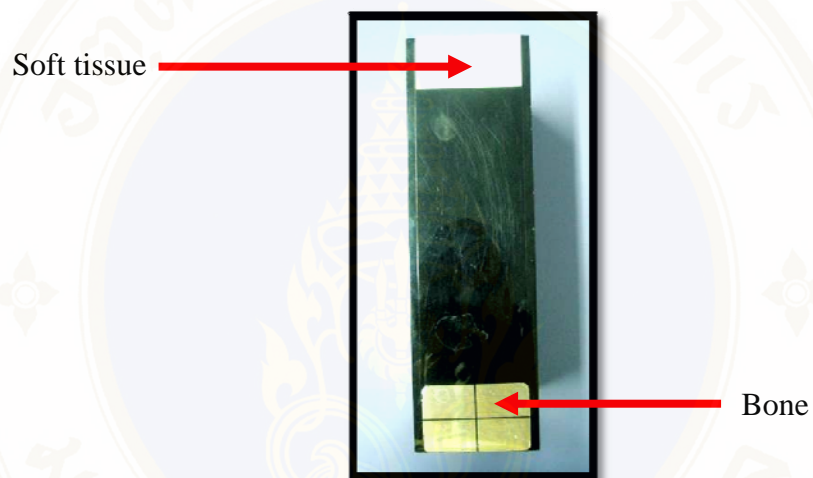


Figure 3.8 Calibration Block (Lunar Prodigy)

3.6.5 Auto region of Interest (ROI) analysis (12)

Hologic Discovery A, W

Correct hip regions of interest for Hologic, with the infero-lateral corner of the femoral neck box anchored to the notch created by the junction of the trochanter and femoral neck and the inferior margin of the total hip 1 cm. below the lower margin of the lesser trochanter (Fig. 3.9).

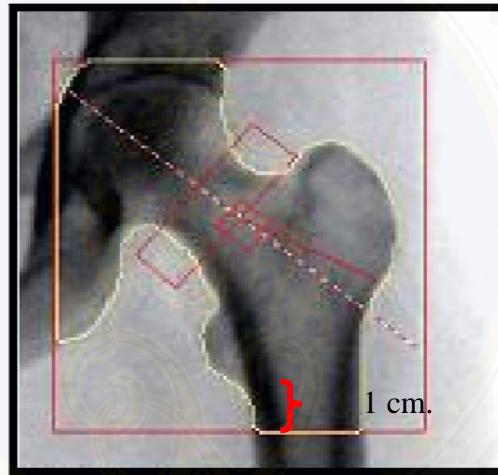


Figure 3.9 Hip's regions of interest for Hologic Discovery A, W

Lunar Prodigy

Correct hip regions of interest for Lunar, with the femoral neck box positioned by the analysis software to be at the narrowest and lowest density region of the neck (approximately midway between the head of the femur and the greater trochanter), and the bottom of the total hip region 5 cm below the junction of the trochanter anchor in ward's region (Fig. 3.10).

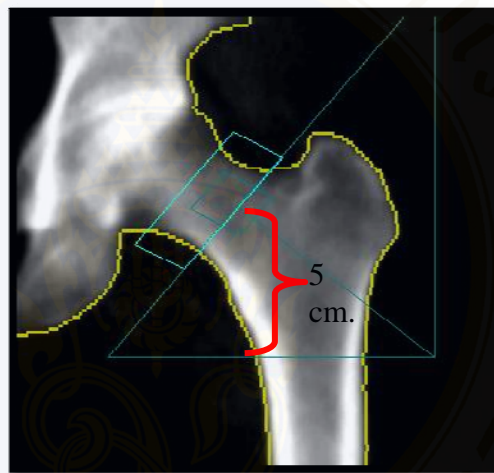


Figure 3.10 Hip's regions of interest for Lunar

3.6.6 Technologist Precision (10)

The LSC was estimated according to the procedure recommended by the International Society for Clinical Densitometry (ISCD) as follows:

- Measure 15 patients 3 times or 30 patients 2 times.
- Measure spine and hip, repositioning the patient after each scan.
- Calculate the root mean square standard deviation (RMS-SD).
- Calculate precision and Least Significant Change, LSC at 95% confidence interval at ROI of Lumbar spine, Total hip and femoral neck

Calculate the root mean square standard deviation (RMS-SD), precision and LSC

1. Standard Deviation (SD)

$$SD = \sqrt{\frac{\sum_{i=1}^n (X_i - \bar{X})^2}{n-1}}$$

where x_i = actual value of the i th measurement

\bar{X} = mean BMD values

n = number of patients

2. Standard Deviation, (Standard Deviation Square)

$$\text{Standard Deviation Square} = SD^2$$

3. Coefficient of Variation (CV)

$$CV = \frac{SD}{\text{Average BMD}}$$

4. Coefficient of Variation, (Coefficient of Variation Square)

$$\text{Coefficient of Variation Square} = CV^2$$

5. Root Mean Square of Standard Deviation, RMS SD

$$RMS\ SD = \sqrt{\frac{\text{sum of } SD\ \text{square}}{n}}$$

6. Coefficient of Variation

$$CV = \sqrt{\frac{\text{sum of } CV\ \text{square}}{n}}$$

7. % Coefficient of Variation = Precision

$$\%CV = CV \times 100$$

8. % Least Significant Change, %LSC

$$\%LSC_{(95\% \text{ Confidence Interval})} = \%CV \times 2.77$$

The minimum acceptable precision for an individual technologist is:

- Lumbar Spine: Percent Coefficient of Variation = 1.9 % (LSC = 5.3 %)
- Total hip: Percent Coefficient of Variation = 1.8 % (LSC = 5 %)
- Femoral Neck: Percent Coefficient of Variation = 2.5 % (LSC = 6.9 %)
- Retraining is required if a technologist's precision is worse than these values

3.7 Position and Analysis (5)

AP Lumbar spine position and Analysis

The recommended positioning and analysis are as follows:

1. Position patient supine, straight and centered on the table pad with hips and shoulders square.
2. Place anatomy to be scanned with the physical limits of the table
3. Positioning block for spine scan (Fig. 3.11)
 - Place the positioning block at the correct angle under the patient's legs.
 - Align edge under the knees
4. Laser light was used to highlight the starting point of the scan; center light on the body about 2 inches below Umbilicus or Iliac crest (Fig. 3.12).



Figure 3.11 AP lumbar spine positioning



Figure 3.12 Laser light position in AP lumbar spine

5. Landmarks and optimal imaging of spine

- Spine straight and centered
- Equal amounts of soft tissue on both side of spine
- Include anatomical landmark: middle of L5 (L5-vertebrae) and middle of T12 (T12-vertebrae)
- L1-L4 clearly separated at the vertebra spaces

6. Lumbar spine Analysis (Fig. 3.13-3.14).

- Use the densitometer software to analyze the scan automatically
- Define bone and soft tissue
- Label vertebral correctly

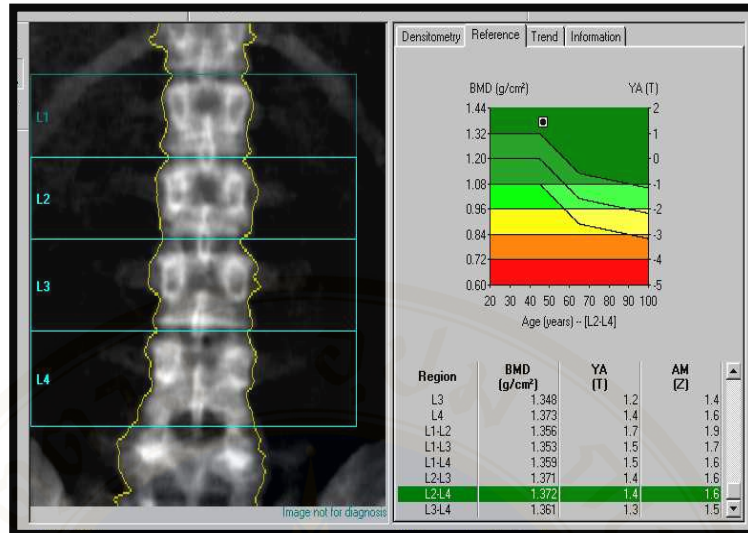


Figure 3.13 AP lumbar spine analysis (Lunar Prodigy)

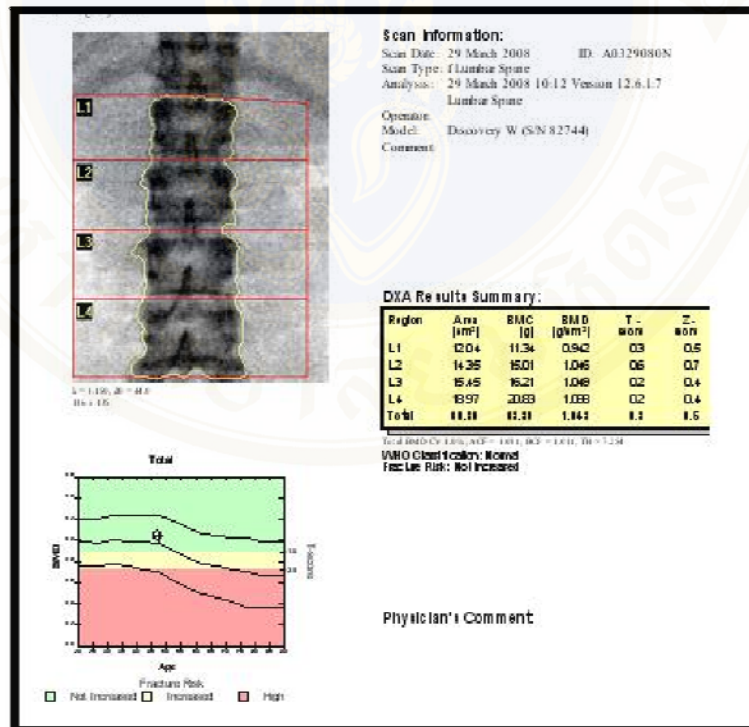


Figure 3.14 AP lumbar spine analysis (Hologic Discovery)

Proximal femur position and analysis (5)

1. Position patient supine, straight and centered on the table pad with hips and shoulders square.
2. Place anatomy to be scanned with the physical limits of the table
3. Position block for femur scan (Fig. 3.15).
 - Place block of femur in center position, with feet together, the femur shaft curves in ward
 - Turn the leg inward between 15-25 degrees
 - Femoral shaft- parallel to the edge of the table
4. Laser light is used to highlight the starting point of the scan; center light on the one hand span below the iliac crest or position laser approximately 7-8 cm. below the greater trochanter (Fig. 3.16).
5. Landmarks and optimal imaging of femur
 - Lesser trochanter
 - Rotate to posterior portion (not visible)
 - Greater trochanter
 - Large, fully visible and separate from femur head by femur neck
 - Femur shaft
 - Straight, perpendicular to the edge of scan box
6. Proximal femur analysis (Fig. 3.17-3.18)
 - Use the software to analyze automatically
 - Adjust the bone edge
 - Neck box must not contain any of greater trochanter

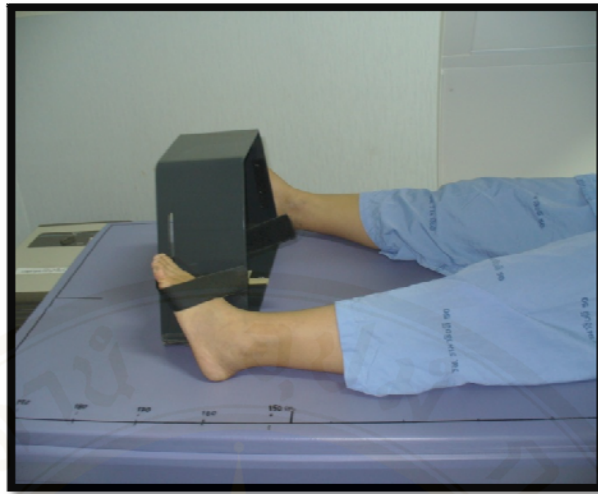


Figure 3.15 Proximal femur positioning

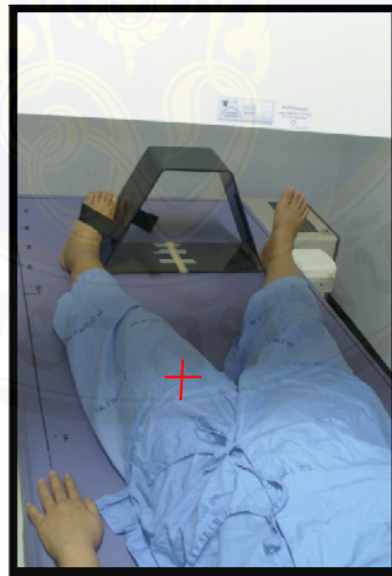


Figure 3.16 Laser light position in proximal femur

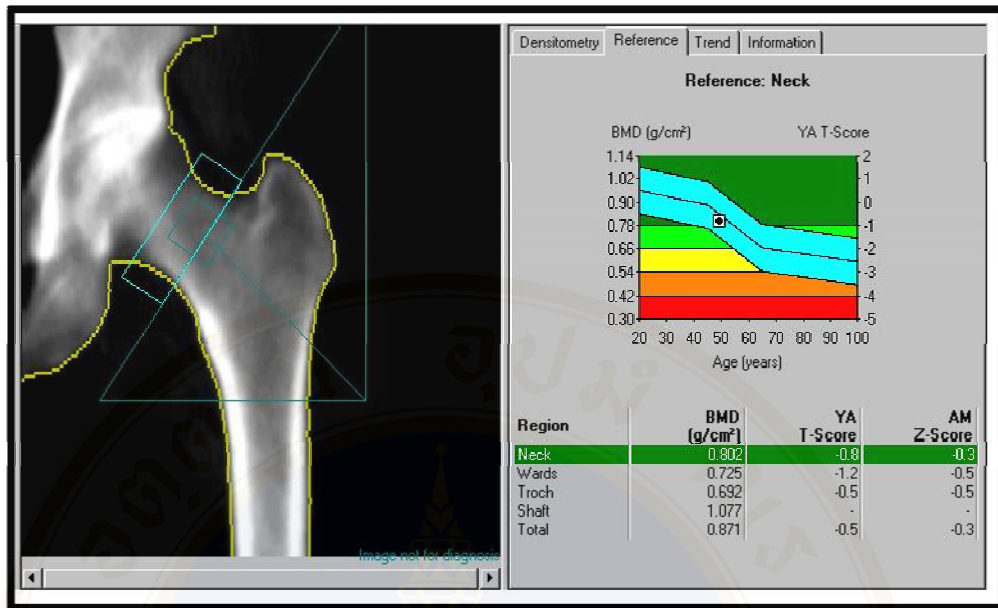


Figure 3.17 Proximal femur analysis (Lunar Prodigy)

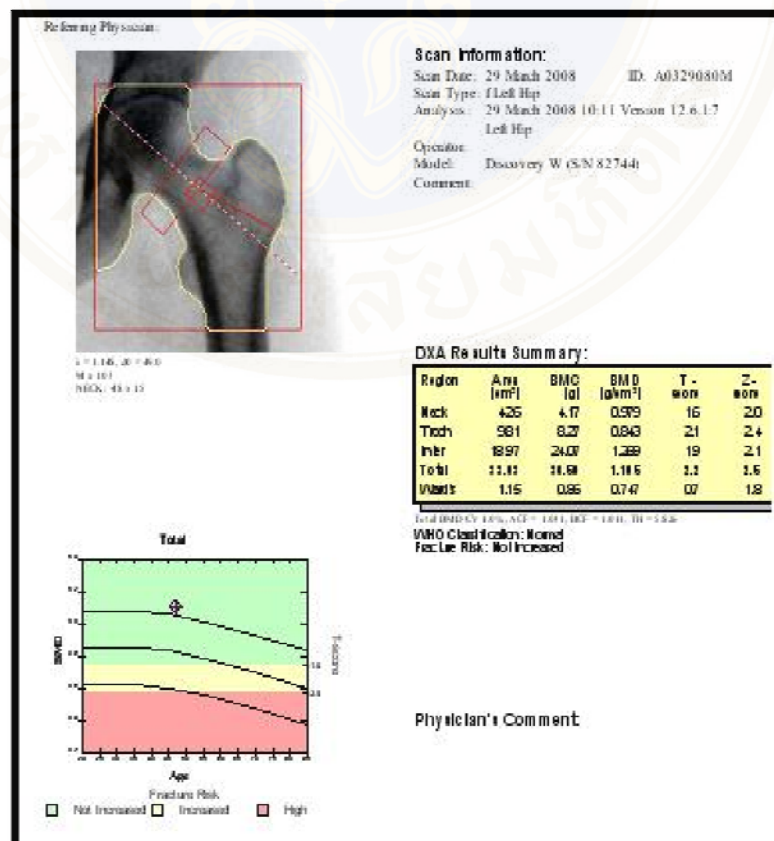


Figure 3.18 Proximal femur analysis (Hologic Discovery)

3.8 The International Society for Clinical Densitometry (ISCD) (13)

The International Society for Clinic Densitometry (ISCD) is a not-for-profit multidisciplinary professional society with a mission to advance excellence in the assessment of skeletal health. This is accomplished by improving knowledge and quality of densitometry among healthcare professionals, educating and certifying clinicians and technologists, increasing patient awareness and access to densitometry, and supporting clinical and scientific advances in the field.

With the evolution of bone densitometry, differences in technologies, acquisition techniques, reference databases, reporting methods, and terminology have developed. These differences may have adverse effects on patient care and the exchange of scientific information. To address these issues, the ISCD periodically holds Position Development Conferences, a process whereby an international panel of experts makes recommendations based on reviews of the scientific literature by task forces associated with the ISCD Scientific Advisory Committee. Recommendations that are approved by the ISCD Board of Directors become Official Positions of the ISCD.

The International Society for Clinic Densitometry (ISCD) is a multidisciplinary, nonprofit organization which was founded in June of 1993 provides a central resource for a number of scientific disciplines with an interest the assessment of skeletal health. The society was the first of its kind worldwide

Membership in ISCD has grown steadily since the organization's inception a standard at nearly 5,000 doctors, technologists, other allied health providers and scientists with an interest in skeletal health. Currently representatives with representation from 30 disciplines including family practice, internal medicine, obstetrics, gynecology, endocrinology, gerontology, nephrology, orthopedics, pediatrics, radiology and rheumatology. In the last several years we have seen impressive growth on to international front. Approximately 10% of our members reside outside the United States in more than 60 countries. In 2008, for the first time international attendees and courses outnumbered their U.S. counterparts. We currently have membership agreements with Brazil, China, France, Taiwan and Korea. Interest

has also been expressed by South Africa, Mexico, Venezuela, Spain, Romania, Sweden, Australia, the Philippines, Indonesia, Colombia, Japan, Poland and Peru.

The ISCD's mission is to advance excellence in the assessment of skeletal health. As such, the ISCD offers comprehensive educational courses in bone densitometry and vertebral fracture assessment (VFA) and certification in dual energy X-ray absorptiometry (DXA) scan acquisition and interpretation for technologists and physicians. Physicians who successfully pass the certification exam are designated Certified Clinical Densitometrists (CCD), while technologists are now designated as Certified Clinical Densitometry Technologists (CBDT). Currently, 7,212 clinicians and 4,361 technologists are ISCD certified world wide.

The International Society for Clinical Densitometry (ISCD) Committee on Standards of Bone Measurement (CSBM) consists of experts in technical aspects of bone densitometry. The CSBM recently reviewed the scientific literature on cross-calibration and precision assessment. A report with recommendations was presented at the 2005 ISCD Position Development Conference (PDC). Based on a thorough review of the data by the ISCD Expert Panel during the conference, the ISCD adopted Official Positions with respect to

1. Cross-calibration when changing or replacing hardware
2. Cross-calibration when an entire system is changed to one made by either the same or a different manufacturer
3. When no cross-calibration study or bone mineral density (BMD) comparison is done between facilities
4. The minimum acceptable precision for an individual technologist.

3.10 Cross-Calibration When Replacing a Whole System for a System with the Same Technology (14)

When changing an entire system to one made by the same manufacturer using a different technology or when changing to a system made by a different manufacturer, one approach to cross-calibration is:

- Scan 30 subjects representative of the facility's patient population once on the initial system and then twice on the new system within 60 days.
- Measure those anatomic sites commonly measured in clinical practice, typically the spine and proximal femur.
- Facilities must comply with locally applicable regulations regarding DXA.
- Calculate the average BMD relationship and Generalized Least Significant Change (GLSC) between the initial and new machine using equation or the ISCD Cross - Calibration Tool.
- Use this Generalized Least Significant Change (GLSC) for comparison between previous and new systems.

3.11 Least significant change (LSC) (15)

The commonly used LSC is defined as the least amount of change between 2 measurements over time that must be exceeded before a change can be considered true (with 95% confidence) as mathematically written in equation 1.. The LSC has clinical applications in monitoring disease progression or treatment effects in bone mineral density (BMD) and bone mineral content.

$$\text{Ideal LSC (ILSC)} = 2.77 * \text{Precision Error} \quad \text{-----} \quad (1)$$

When a patient’s BMD is measured on different DXA systems, Equation 1 cannot be assumed to be valid since the 2 systems may have different precisions and calibrations. The ILSC also does not take into account other effects that would decrease the correlation between the 2 systems, including differences in regions of interests, differences in X-ray techniques and detection technologies and different bone edge detection algorithms

The LSC concept has only been applied to comparisons of bone mineral density (BMD) values taken on the same or identical systems. Quantitative comparisons between bone densitometers of different make and manufacturer have neither been straight forward nor recommended because of the loss of confidence that the differences between BMD values were real and not due to calibration differences. Until recently, clinicians did not have the ability to quant if the 95% confidence interval between 2 scans in this condition. A recent article described a method to cross-calibrate 2 systems of different technology and create a LSC referred to as the generalized least significant change (GLSC). As show in equation 2.

$$\text{GLSC} = 1.96 \sqrt{\hat{\sigma}_Y^2 + \frac{(n-1)}{(n-2)} S_Y^2 (1 - \hat{r}^2) \left(1 + \frac{1}{n} + \frac{S_X^2 + (\hat{\sigma}_X^2 - S_X^2)}{(n-1) S_X^2} \right)} + \hat{b}^2 \hat{\sigma}_X^2 \quad \text{--- (2)}$$

Where:

- Old system (System 1) = X
- New system (System 2) = Y
- Precision of old system = σ_x
- Precision of new system = σ_y
- Variances of cross-calibration population of old system = S_x
- Variances of cross-calibration population of new system = S_y
- Regression slope = b
- Correlation coefficient = r
- Number of subject = n

A. Shepherd et al. studied A Generalized Least Significant Change for Individuals Measured on different DXA system (15)

These were the 2 most popular bone densitometer systems on the market at this writing. As part of a larger study, each participant had duplicate left hip and spine scans on each systems. This protocol resulted in a data set for calculating the GLSC with precision and accuracy measured on each system on the same individuals. Figure 3.35 shows the results from this cross-calibration and precision study in a form to be used by Eq. (2). Twenty-nine participants were scanned but 1 subject was excluded because of unidentifiable bone artifacts in the hip.

Variable	Description	Spine	Total hip	Neck
n	Number of subjects	29	29	29
r	Correlation coefficient	0.9804	0.9749	0.9207
a	Regression intercept	0	0	0
b	Regression slope (Delphi = Prodigy*b)	0.8313	0.9790	0.8078
σ_x	Precision of Prodigy (g/cm^2)	0.0095	0.0066	0.0116
σ_y	Precision of Delphi (g/cm^2)	0.0116	0.0130	0.0147
RMSE(\sqrt{MSE})	Root mean square error or standard error of the estimate (g/cm^2)	0.0316	0.0288	0.0418
S_x	Population standard deviation on Prodigy (g/cm^2)	0.1860	0.1263	0.1198
S_y	Population standard deviation on Delphi (g/cm^2)	0.1577	0.1268	0.1051
μ_x	Population mean on Prodigy (g/cm^2)	1.1246	0.9013	0.8609
μ_y	Population mean on Delphi (g/cm^2)	0.9349	0.8824	0.6954
ILSC _x	ILSC on Prodigy (g/cm^2)	0.026	0.018	0.032
%ILSC _x	ILSC on Prodigy (%)	2.31%	2.00%	3.72%
ILSC _y	ILSC on Delphi (g/cm^2)	0.032	0.036	0.041
%ILSC _y	ILSC on Delphi (%)	4.33%	3.31%	4.37%
GLSC _x	GLSC from Prodigy to Delphi (g/cm^2)	0.070	0.065	0.091
%GLSC _x	GLSC from Prodigy to Delphi (%)	7.1%	6.8%	12.5%
GLSC _y	GLSC from Delphi to Prodigy (g/cm^2)	0.083	0.065	0.105
%GLSC _y	GLSC from Delphi to Prodigy (%)	7.3%	7.2%	12.2%

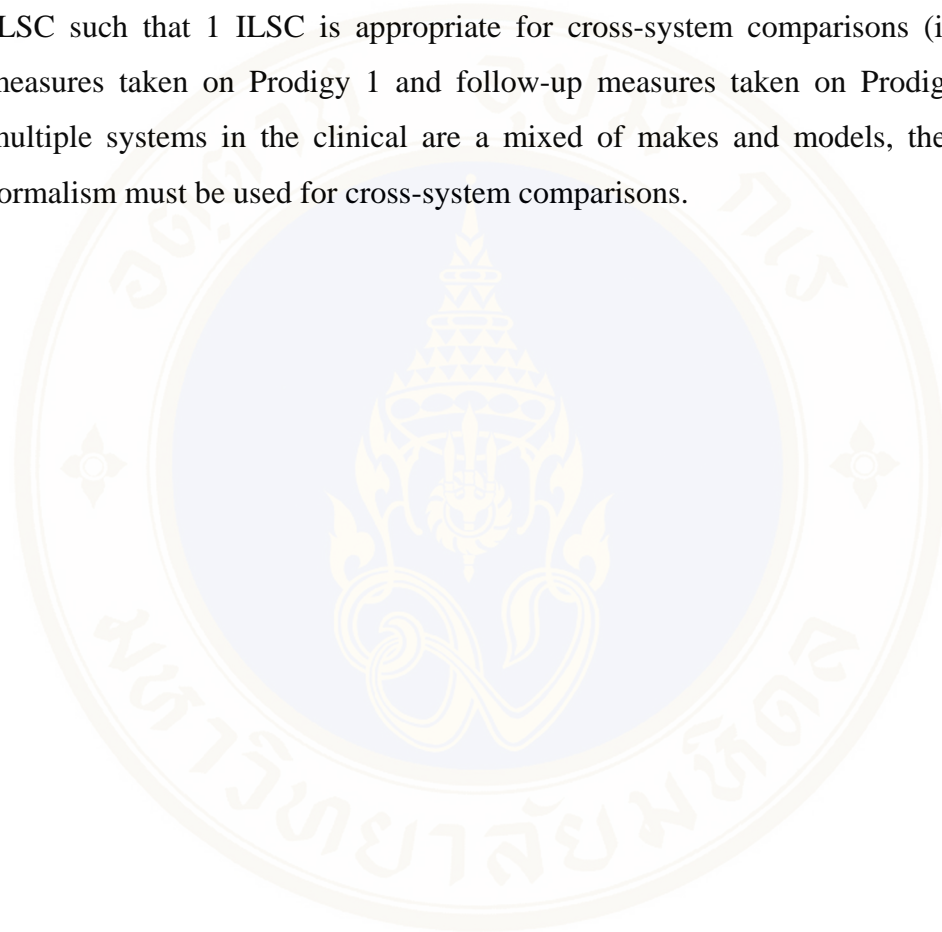
Abbr: LSC, least significant change; ILSC, ideal least significant change; GLSC, generalized least significant change.

Figure 3.19 Result of cross-calibration between Hologic Delphi and Lunar Prodigy (15)

Figure 3.19 displays the results of Cross-Calibration Study between the Hologic Delphi and GE Lunar Prodigy in the Form of Input to Equation 2. We see that the GLSC is substantially worse than the ILSC when scans are acquired on systems from 2 manufacturers. If quantitative comparisons were done with a Prodigy baseline scan and a Delphi follow-up scan, the GLSC would be larger than the LSC of the Prodigy alone by 2.6, 3.6, and 2.8 times for the spine, total hip, and neck, respectively.

If the magnitude of the difference between a patient’s baseline BMD measure on system 1 and their follow-up BMD measure on system 2 is greater than the GLSC, then there is 95% confidence that a true change in BMD has occurred.

The GLSC can also be used when comparing measures between multiple systems within a clinic. For example, it is common in larger imaging centers to have more than 1 DXA systems. Without the GLSC, one cannot compare results between the systems and assign subjects to the first available DXA system. If multiple systems are all of the same make and model, we have shown how the GLSC may reduce to the ILSC such that 1 ILSC is appropriate for cross-system comparisons (i.e., baseline measures taken on Prodigy 1 and follow-up measures taken on Prodigy 2). If the multiple systems in the clinical are a mixed of makes and models, the full GLSC formalism must be used for cross-system comparisons.



3.12 Optimum Number of Participants for a Cross-Calibration Study

(15)

A. Shepherd et al. studied in A Generalized Least Significant Change for Individuals Measured on different DXA system. They measure bone mineral density of 10,000 subjects by DXA 2 systems.

There are very few input parameters in Eq.(2) that can be optimized. Most are the characteristics of the systems and patient population.

As demounts rated, increasing then from 10 (GLSC = 0.0475, 2.21 times the ILSC) to infinity (the asymptotic GLSC = 0.0420, 1.96 times the ILSC) only decreases the GLSC by 12.7% (Fig. 3.20).

If we use $n = 30$, as suggested by the ISCD, we have GLSC of 0.0437, only 4% away from 0.0420. Thus, considering the time and effort, there is little to be gained in reducing the magnitude of the GLSC by including more than 30 participants in a cross-calibration study.

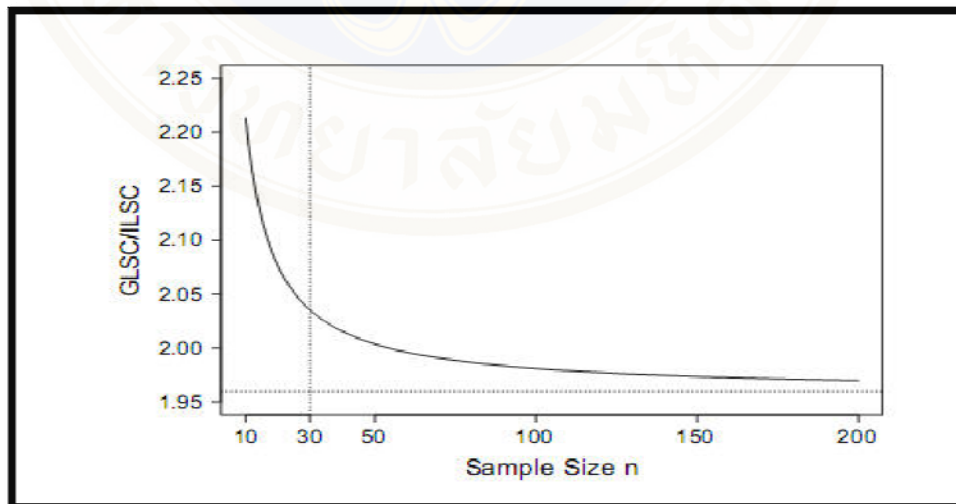


Figure 3.20 Relationship between number of sample size and magnitude of GLSC

CHAPTER IV

MATERIALS AND METHODS

4.1 Materials

4.1.1 Three DXA systems

- Lunar Prodigy
- Hologic Discovery A
- Hologic Discovery W

4.1.2 Subjects

Patients aged at least 20 years old sent for DXA examination at Nuclear Medicine Unit, Ramathibodi Hospital were invited to participate in the study. Thirty females who gave written informed consent (Appendix B) after being explained and reading the volunteer information sheet (Appendix C) about the study were included.

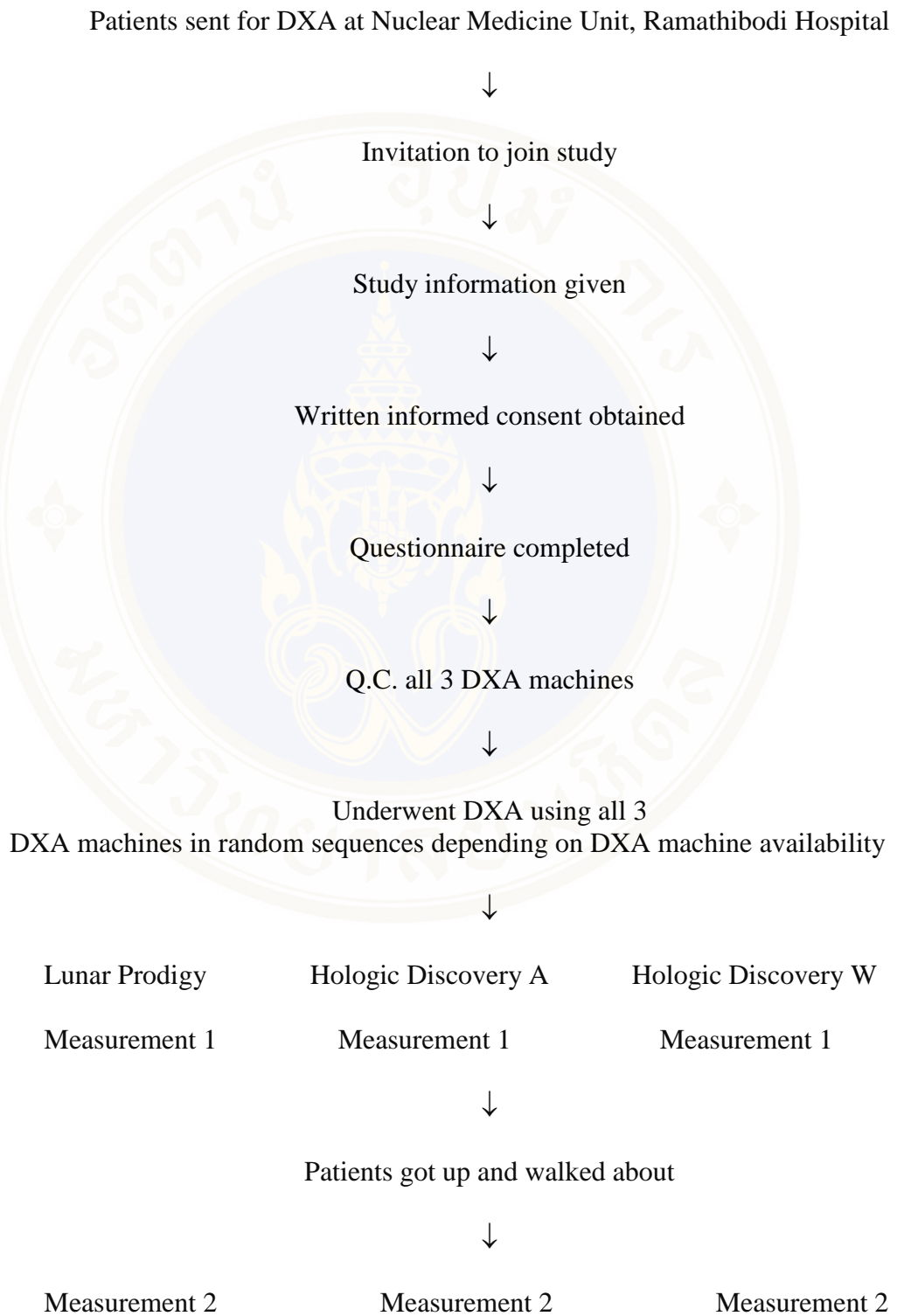
Exclusion criterion

The subjects were excluded from the study if there was a structural abnormality or artifact at any measurement sites (L1-L4 vertebrae or hip) rendering DXA assessment inaccurate.

4.2 Methods

The protocol of the study was approved by the institutional review board. The subjects completed the questionnaire (Appendix D) and underwent BMD measurements at the lumbar spine and proximal femur using all 3 DXA machines (Lunar Prodigy, Hologic Discovery A, and Hologic Discovery W) in random sequences depending on the availability of the machine at the time. With each machine, each site was measured twice with repositioning. The repositioning was done after the subjects had undergone the first measurement, got up from the imaging table, walked about in front of the imaging room, and returned to the imaging table for a second measurement to simulate as close as possible the setting of the follow-up DXA scan.

Diagram of Study Procedure



Quality control for DXA

The Quality Control (Q.C.) program at our DXA facility strictly adheres to manufacturer guidelines for system maintenance as follows:

- Perform periodic (at least once per week) phantom scans for any DXA system as an independent assessment of system calibration.
- Plot and review data from calibration and phantom scans.
- Verify the phantom mean BMD after any service performed on the densitometer.
- Establish and enforce corrective action thresholds that trigger a call for service.
- Maintain service logs.
- Comply with government inspections, radiation surveys and regulatory requirements.

Quality Control for Hologic Discovery

Daily QC procedure

Place the spine phantom (Fig. 4.2) on the imaging table at the position marked by the manufacturer and start scanning (Fig. 4.3). The BMC, area scanned and calculated BMD of the spine phantom were generated and plotted automatically. The DXA machine is considered functioning acceptably when all BMC, area and BMD fall within 1.5% mean value at calibration (Fig. 4.4-4.5).



Figure 4.1 Hologic Discovery and Console

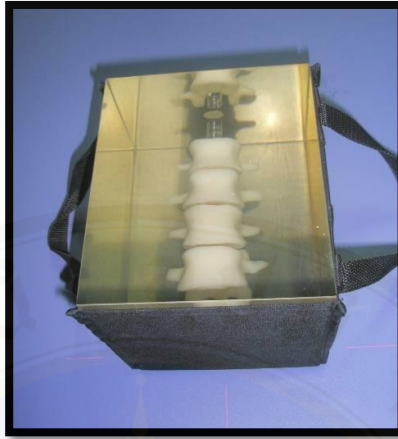


Figure 4.2 Spine Phantom



Figure 4.3 Position of Hologic spine phantom

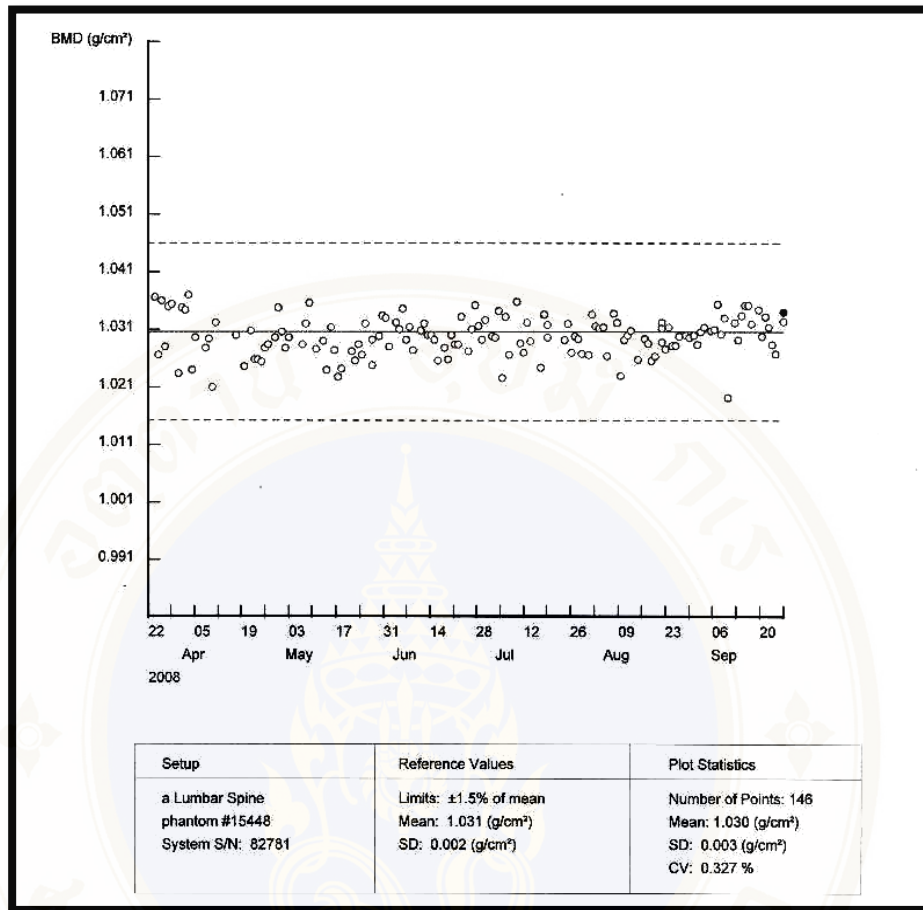


Figure 4.5 Hologic Discovery daily Q.C. data Plot

Quality Control for Lunar Prodigy

Daily Q.C. procedure

1. Calibration Block (Fig. 4.7)
2. Aluminum Spine Phantom (Fig. 4.8)



Figure 4.6 Lunar Prodigy



Figure 4.7 Calibration Block



Figure 4.8 Aluminum Spine Phantom

Calibration Block procedure

1. Position of calibration block (Fig. 4.9) at the site marked by the manufacturer and start scanning.



Figure 4.9 Position of Calibration Block in the daily Q.C.

2. Automatic Function test and Secondary calibration
3. Automatic record and display result (Fig. 4.10)

Functional Tests			Secondary Calibration			
Test	Value	Status	Test	Mean	% CV	Status
Peaking	2,343	Pass	BMD			
Beam Stop	0.42 / 0.33	Pass	Large	1.504	0.2%	Pass
Mechanical Test			Medium	1.005	0.3%	Pass
Transverse	622.83	Pass	Small	0.504	1.0%	Pass
Longitudinal	1,988.70	Pass	Tissue			
Spillover Test			Lean	8.1%	2.8%	Pass
Mean %	7.88%	Pass	Mid	36.6%	0.4%	Pass
Stability	0.00%	Pass	Fat	62.1%	0.4%	Pass
Reference Counts			Calibration Status			Pass
High mA	154,191 / 182,361	Pass	System Status			
Ratio at High mA	0.85	Pass	Pass			
Detector Status		Pass				

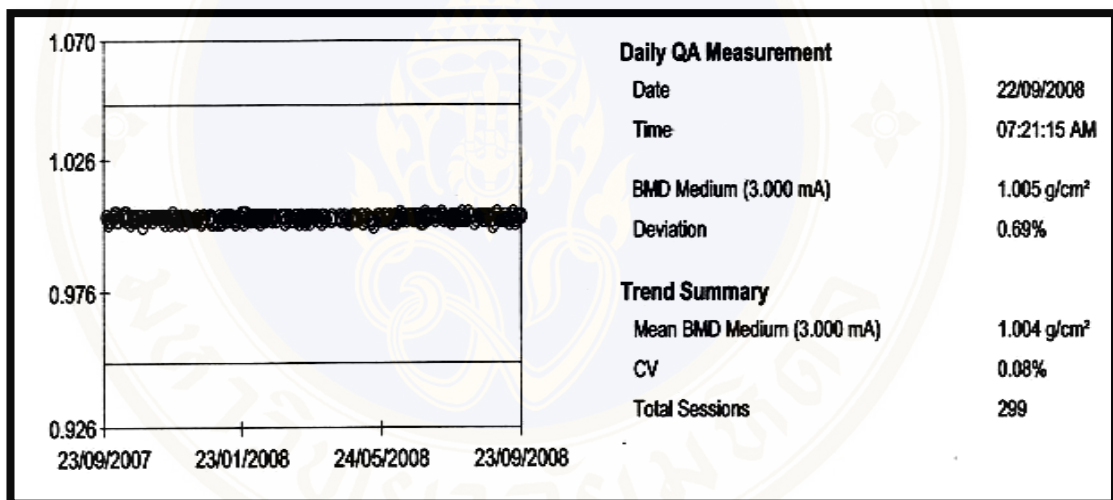


Figure 4.10 Result of daily Q.C.

Aluminum Spine Phantom procedure

Place Aluminum Spine Phantom at the sited marked by the manufacturer (Fig. 4.11) and scan the phantom 10 times. The software automatically generates the spine ROI, which may need some adjustment to properly delineate the phantom vertebrae prior to routine reading by the software. The resulting BMD should not exceed $\pm 1.5\%$ of mean value at calibration (Fig. 4.12).

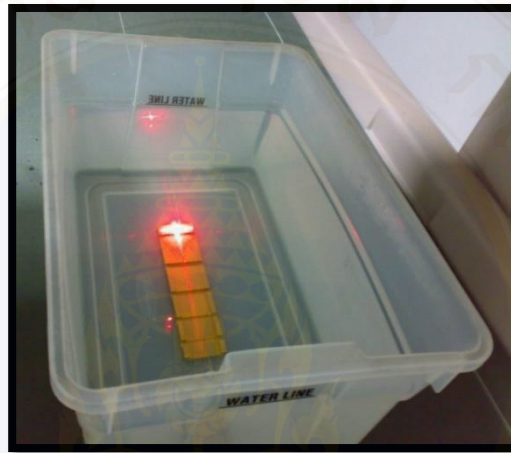


Figure 4.11 Laser and spine phantom in daily Q.C. Lunar Prodigy

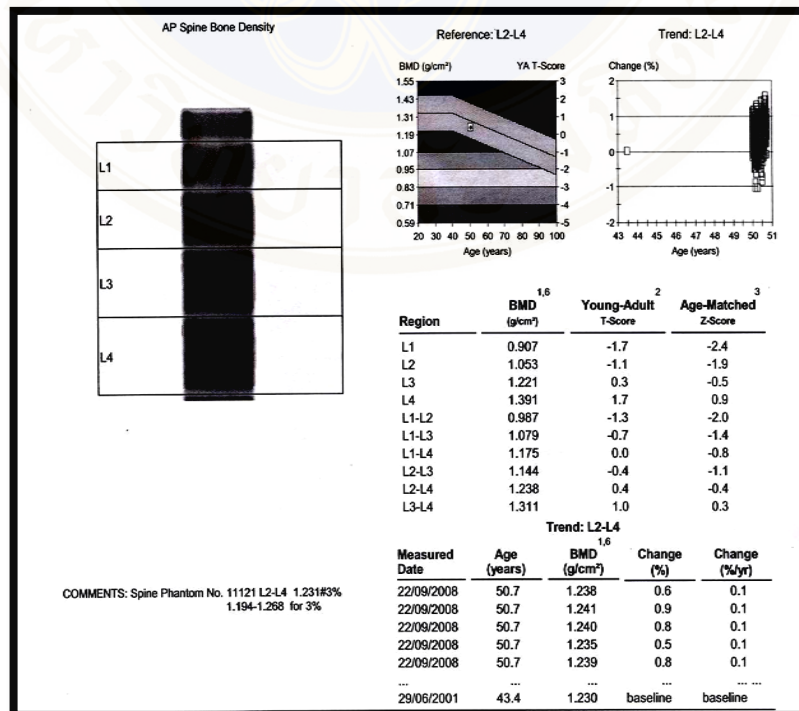


Figure 4.12 Lunar Prodigy Daily Q.C. data

Patient positioning and BMD analysis

Proximal femur BMD

Each volunteer lied supine with the trunk straight, and centered on the imaging table pad. The hips and shoulders squared. A position block for femur scan provided by the relevant manufacturer was placed in the center position. Then the volunteer's foot was placed attached to the block according to the manufacturer manual so that the hip and leg were internally rotated 15-25 degrees such that the hip was centered on the imaging table and the femoral shaft was straight and parallel to the edge of the table.

The laser light was used to mark the starting point of the scan, covering from one hand breadth below the iliac crest.

The manufacturer software was used to analyze the BMD at the femoral neck and total hip. Automated regions of interest (ROIs) were generated for both femoral neck and total hip. The observer corrected the ROIs if they did not delineate the measurement sites properly, i.e. no inclusion of soft tissue, artifact, or abnormal calcification. The procedure followed the manufacturer manual.

Lumbar spine BMD

On supine position with the shoulders and hips squared, the patient's legs were placed on the manufacturer positioning block such that the lumbar spine lay flat on the imaging table without being tilted due to lumbar lordosis. The lumbar spine was straight and centered with equal amount of soft tissue on both sides of the spine. The visualized part included the middle vertebral body of T12 to L5 vertebra. Each lumbar vertebra was clearly separated at inter-vertebral spaces.

Calculate Generalized Least Significant Change and compare cross calibration equation from this research and cross calibration equation from manufacturer.

Calculate Generalized Least Significant Change between the system 1 and system2 using equation 2 between DXA (Dual Energy X-ray Absorptiometry) Lunar Prodigy, Hologic Discovery A and Hologic Discovery W in lumbar spine, neck of femur and total hip. The machine in system1 and system 2 are listed in table 4.1

Table 4.1 Machine in system 1 and system 2

System 1	System 2
Lunar Model Prodigy	Hologic Model Discovery A
Lunar Model Prodigy	Hologic Model Discovery W
Hologic Model Discovery A	Hologic Model Discovery W

Plot curve and calculate relationship between BMDs of system1 and system2 at lumbar spine, neck of femur and total hip in order to generate cross calibration equation.

Compare cross calibration equation from this research and cross calibration equation from manufacturer.

- Random BMDs (16) from first or second measurement for system 1 (lumbar spine, total hip and neck of femur)
- Use cross calibration equation (research) to predicted BMDs from system 1 (random BMD) to system 2
- Compare BMD between predicted BMDs from research cross calibration equation and actual measurement from system 2

- Use Bland & Altman plot reveal a relationship between difference (BMD_{predicted} and BMD_{observed}) and mean of BMD (BMD_{predicted} and BMD_{observed})

$$\text{Mean} = \frac{\text{BMD}_p + \text{BMD}_o}{2}$$

$$\text{Difference} = \text{BMD}_o - \text{BMD}_p$$

: BMD_{predicted} (BMD_p) = BMD from cross calibration equation (research)

: BMD_{observed} (BMD_o) = BMD from actual measurement in system 2

- Plot curve between difference and mean

- Calculate 95% limits of agreement (14) of BMD

$$\text{Mean Difference} = \frac{\sum \text{Difference}}{30}$$

$$\text{SD Difference} = \sqrt{\frac{\sum_{i=1}^n (\text{Diff}_i - \overline{\text{Diff}})^2}{n-1}}$$

- Upper 95% limits of agreement

$$= \text{Mean Difference} + (1.96 \times \text{SD Difference})$$

- Lower 95% limits of agreement

$$= \text{Mean Difference} - (1.96 \times \text{SD Difference})$$

- Use cross calibration equation (manufacturer) to predicted BMDs from system 1 (random BMD) to system 2

- Compare BMDs between predicted BMDs from manufacturer cross calibration equation and actual measurement from system 2

- Use Bland & Altman plot reveal a relationship between difference (BMD_{predicted} and BMD_{observed}) and mean of BMD (BMD_{predicted} and BMD_{observed})

- Plot curve between difference and mean

- Calculate 95% limits of agreement of BMD

- Compare 95% limits of agreement between research and manufacturer cross calibration equation

CHAPTER V

RESULTS

The volunteer's characteristics were shown in table 5.1

Table 5.1 Volunteer's characteristics

	Mean \pm S.D.
Age (years)	55.161 \pm 8.622
Weight (kg.)	59.558 \pm 8.521
Height (cm.)	152.806 \pm 6.065

1. Generalized Least Significant Change of DXA from Lunar Prodigy, Hologic Discovery A and W at division of Nuclear Medicine, Ramathibodi Hospital were shown in table 5.2.

Table 5.2 GLSC from system 1 to system 2

	Lumbar spine	Neck of femur	Total hip
Lunar Prodigy \rightarrow Hologic Discovery A			
GLSC (g/cm^2)	0.066	0.088	0.066
%CV GLSC	7.2	12.5	7.9
Lunar Prodigy \rightarrow Hologic Discovery W			
GLSC (g/cm^2)	0.064	0.076	0.070
%CV GLSC	7.3	10.8	8.3
Hologic Discovery A \rightarrow Hologic Discovery W			
GLSC (g/cm^2)	0.020	0.074	0.062
%CV GLSC	2.2	10.4	7.3

2. Cross calibration equations from this research shown in the table 5.3-5.5.

Table 5.3 Cross calibration equation between Lunar Prodigy and Hologic Discovery A

ROI	Equation
Lumbar spine	Hologic Discovery A = (-0.008) + (0.875 * Lunar Prodigy)
Neck of femur	Hologic Discovery A = (-0.018) + (0.848 * Lunar Prodigy)
Total hip	Hologic Discovery A = (0.043) + (0.848 * Lunar Prodigy)

Table 5.4 Cross calibration equation between Lunar Prodigy and Hologic Discovery W

ROI	Equation
Lumbar spine	Hologic Discovery W = (-0.044) + (0.881 * Lunar Prodigy)
Neck of femur	Hologic Discovery W = (-0.056) + (0.900 * Lunar Prodigy)
Total hip	Hologic Discovery W = (-0.033) + (0.945 * Lunar Prodigy)

Table 5.5 Cross calibration equation between Hologic Discovery A and Hologic Discovery W

ROI	Equation
Lumbar spine	Hologic Discovery W)= (-0.029) + (1 * Hologic Discovery A)
Neck of femur	Hologic Discovery W)= (0.003) + (1.003 * Hologic Discovery A)
Total hip	Hologic Discovery W)= (-0.057) + (1.086 * Hologic Discovery A)

3. The research gives the comparison between research’s cross calibration equations and manufacturer’s cross calibration equations

Manufacturer cross calibration equations

- Lunar Prodigy and Hologic Discovery A,W

$$\text{Hologic Discovery A, W} = (-0.038) + (0.918 * \text{Lunar Prodigy})$$
- Hologic Discovery A and Hologic Discovery W

$$\text{Hologic Discovery W} = (0) + (1 * \text{Hologic Discovery A})$$

3.1 The comparison between Lunar Prodigy and Hologic Discovery A were shown in table 5.6 . The Plot of mean and difference Altman and Bland between research’s cross calibration equations vs. manufacturer’s cross calibration equations in Lunar Prodigy and Hologic Discovery A at the lumbar spine were shown in Figure 5.1 the neck of femur were shown in Figure 5.2 and the total hip were shown in Figure 5.3

Table 5.6 95% confidence interval of difference between observed and predicted BMD using research equations and manufacturer equations (cross calibration equations between Lunar Prodigy and Hologic Discovery A)

	Research Equations	Manufacturer Equations
	95% confidence interval	95% confidence interval
Lumbar spine	-0.0507 - 0.0492	-0.0678 - 0.0359
Neck of femur	-0.0778 - 0.0864	-0.0705 - 0.0944
Total hip	-0.0569 - 0.0534	-0.1003 - 0.0269

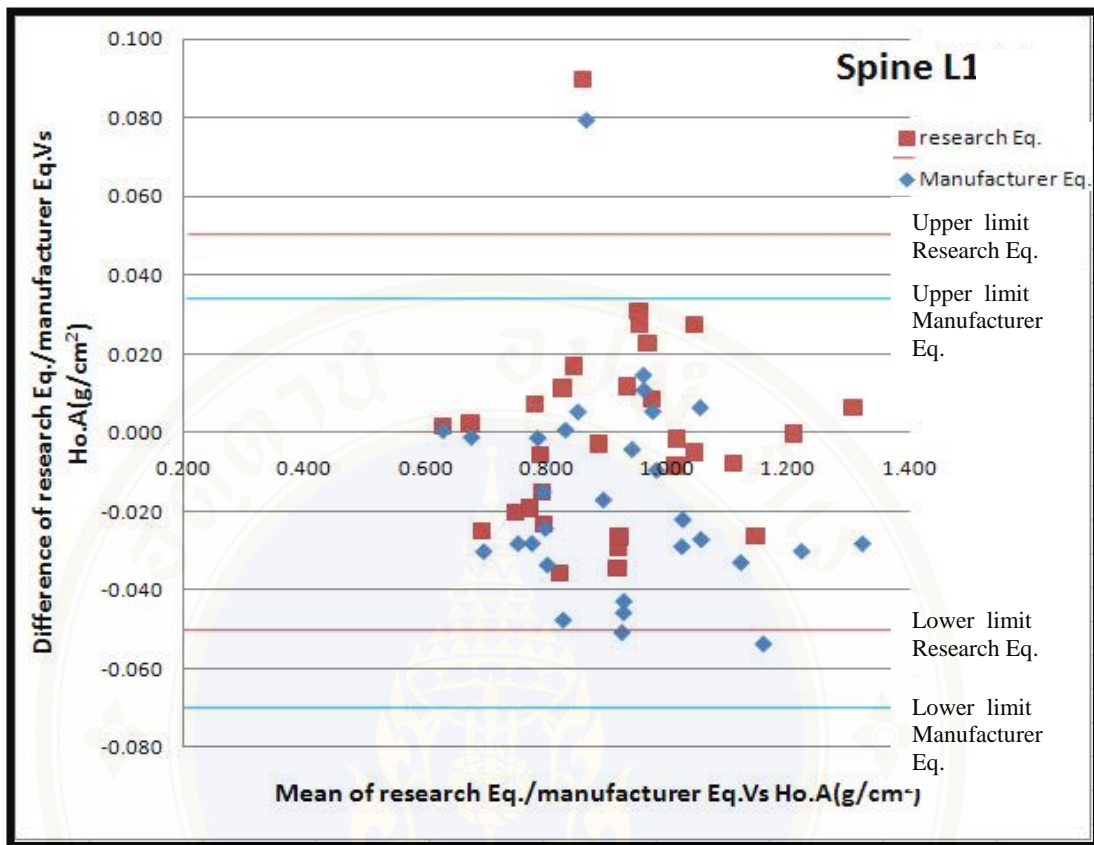


Figure 5.1 Plot of mean and difference Altman and Bland between research’s cross calibration equations vs. manufacturer’s cross calibration equations in Lunar Prodigy and Hologic Discovery A at the lumbar spine

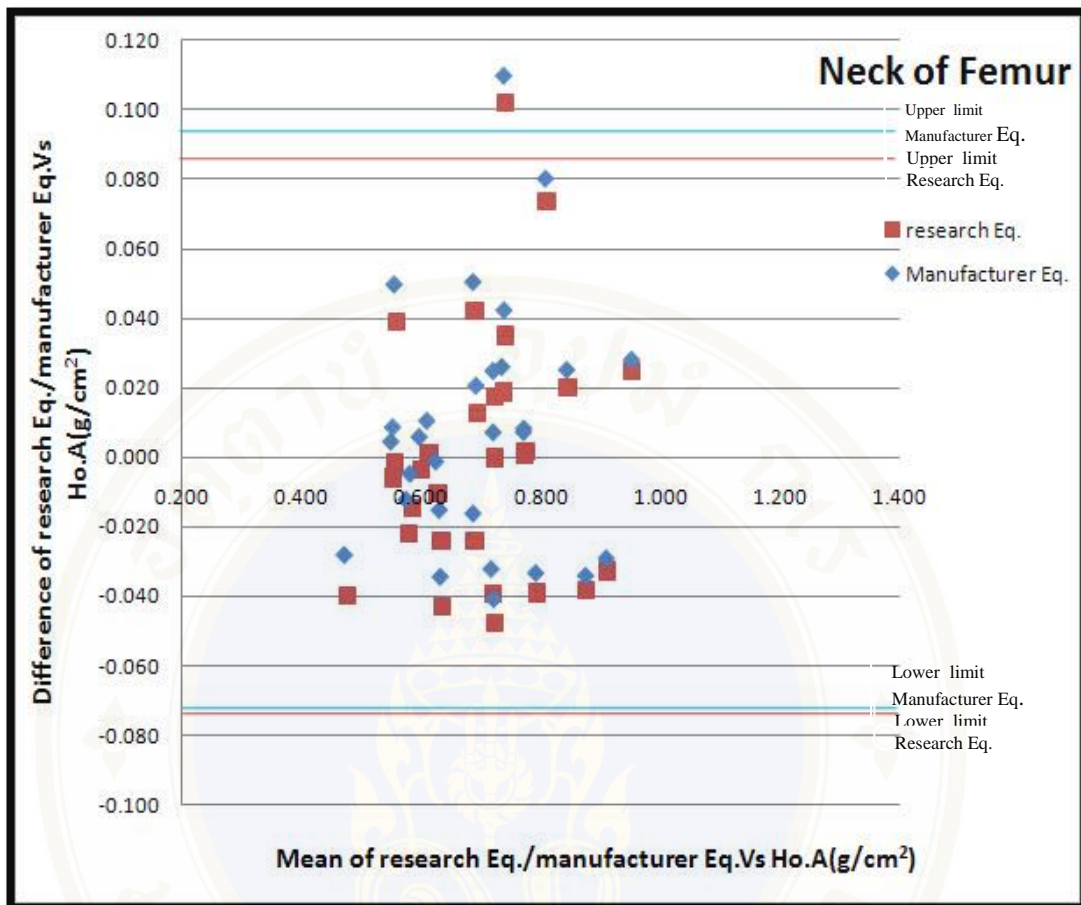


Figure 5.2 Plot of mean and difference Altman and Bland between research’s cross calibration equations vs. manufacturer’s cross calibration equations in Lunar Prodigy and Hologic Discovery A at the neck of femur

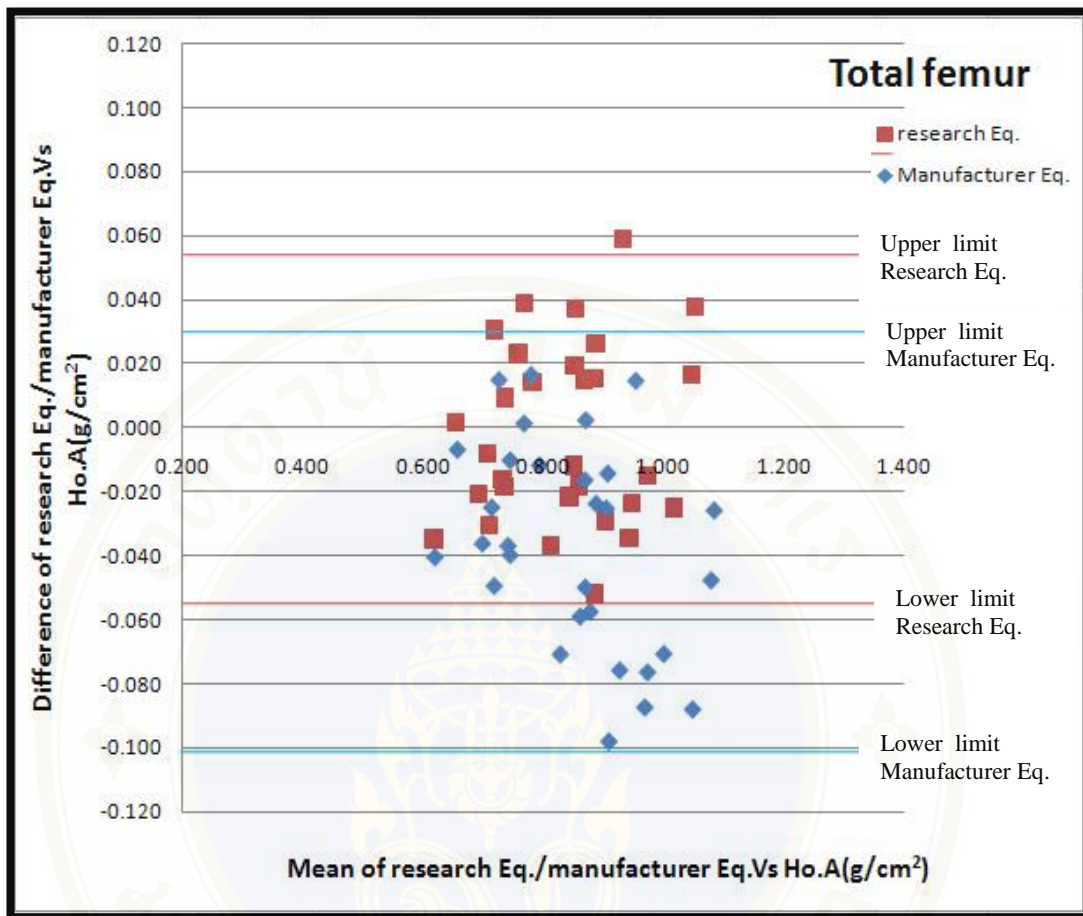


Figure 5.3 Plot of mean and difference Altman and Bland between research’s cross calibration equations vs. manufacturer’s cross calibration equations in Lunar Prodigy and Hologic Discovery A at the total hip

3.2 The comparison between Lunar Prodigy and Hologic Discovery W were shown in table 5.7 The Plot of mean and difference Altman and Bland between research's cross calibration equations vs. manufacturer's cross calibration equations in Lunar Prodigy and Hologic Discovery W at the lumbar spine were shown in Figure 5.4 the neck of femur were shown in Figure 5.5 and the total hip were shown in Figure 5.6

Table 5.7 95% confidence interval of difference between observed and predicted BMD using research equations and manufacturer equations (cross calibration equations between Lunar Prodigy and Hologic Discovery W)

	Research Equations	Manufacturer Equations
	95% confidence interval	95% confidence interval
Lumbar spine	-0.0515 - 0.0512	-0.0986 - 0.0085
Neck of femur	-0.0731 - 0.0679	-0.0591 - 0.0811
Total hip	-0.0643 - 0.0562	-0.0854 - 0.0367

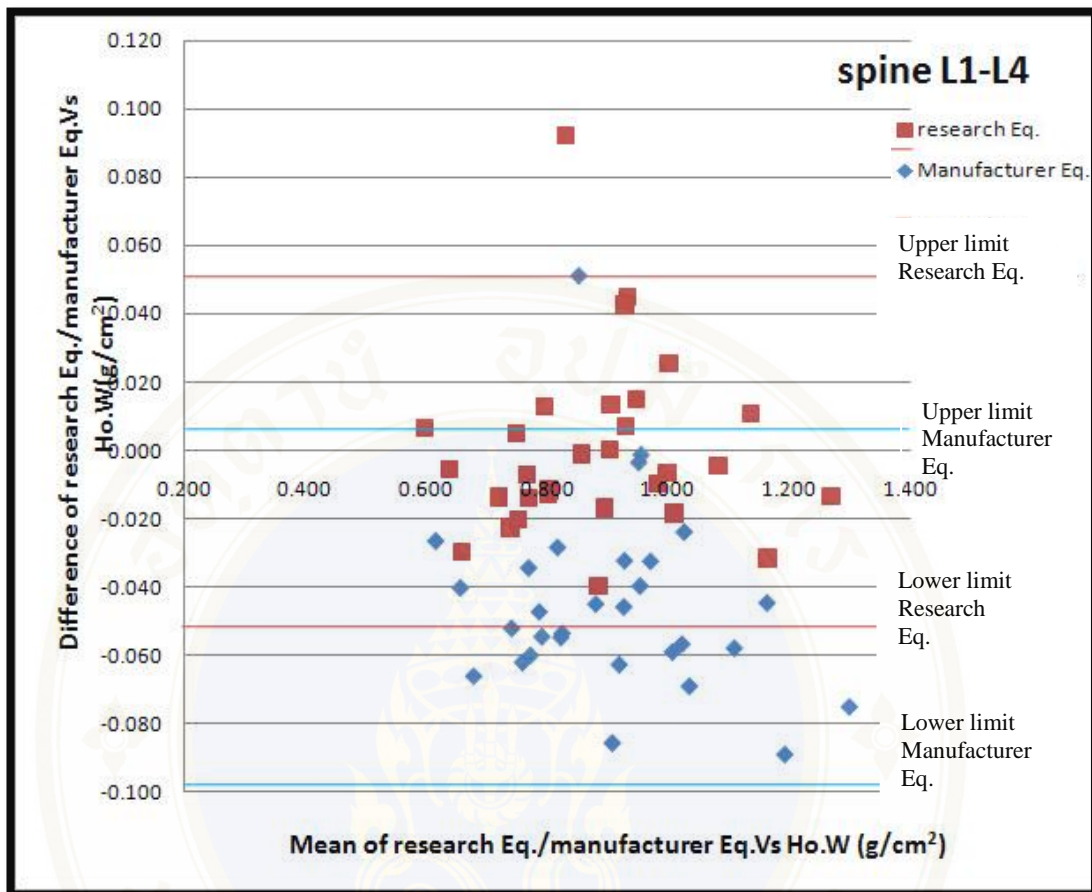


Figure 5.4 Plot of mean and difference Altman and Bland between research’s cross calibration equations vs. manufacturer’s cross calibration equations in Lunar Prodigy and Hologic Discovery W at the lumbar spine

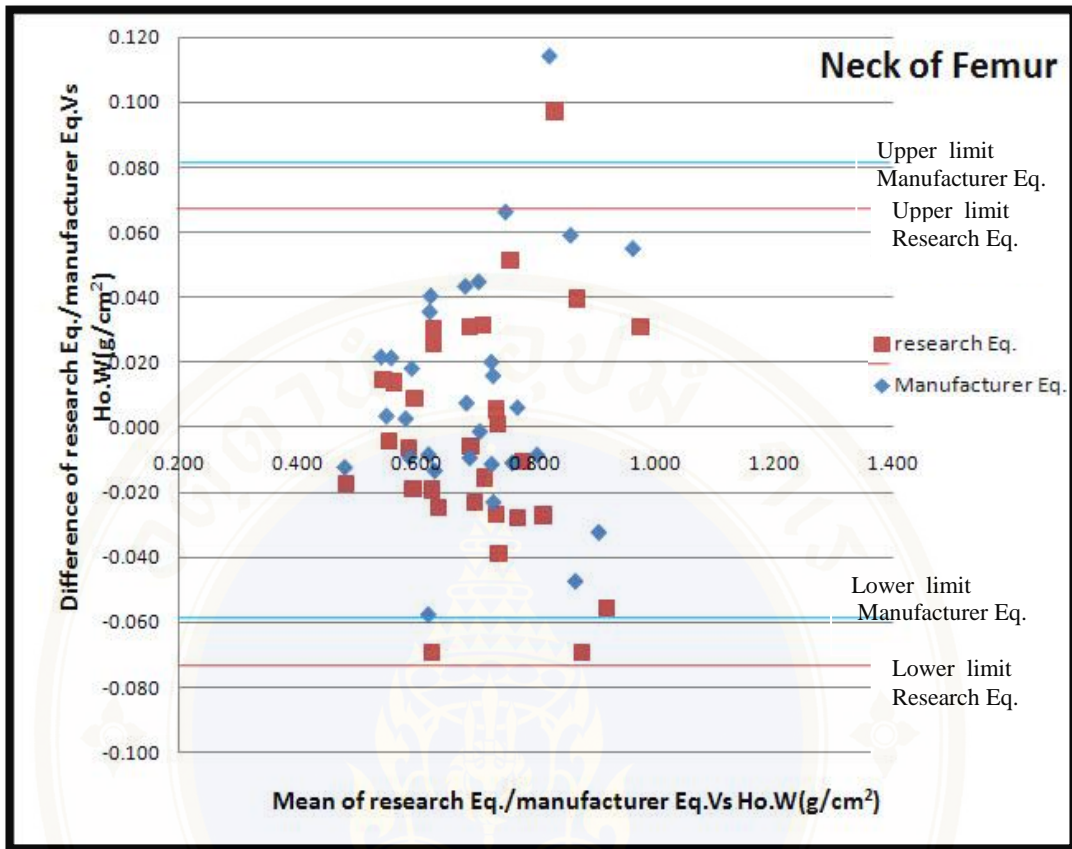


Figure 5.5 Plot of mean and difference Altman and Bland between research’s cross calibration equations vs. manufacturer’s cross calibration equations in Lunar Prodigy and Hologic Discovery W at the neck of femur

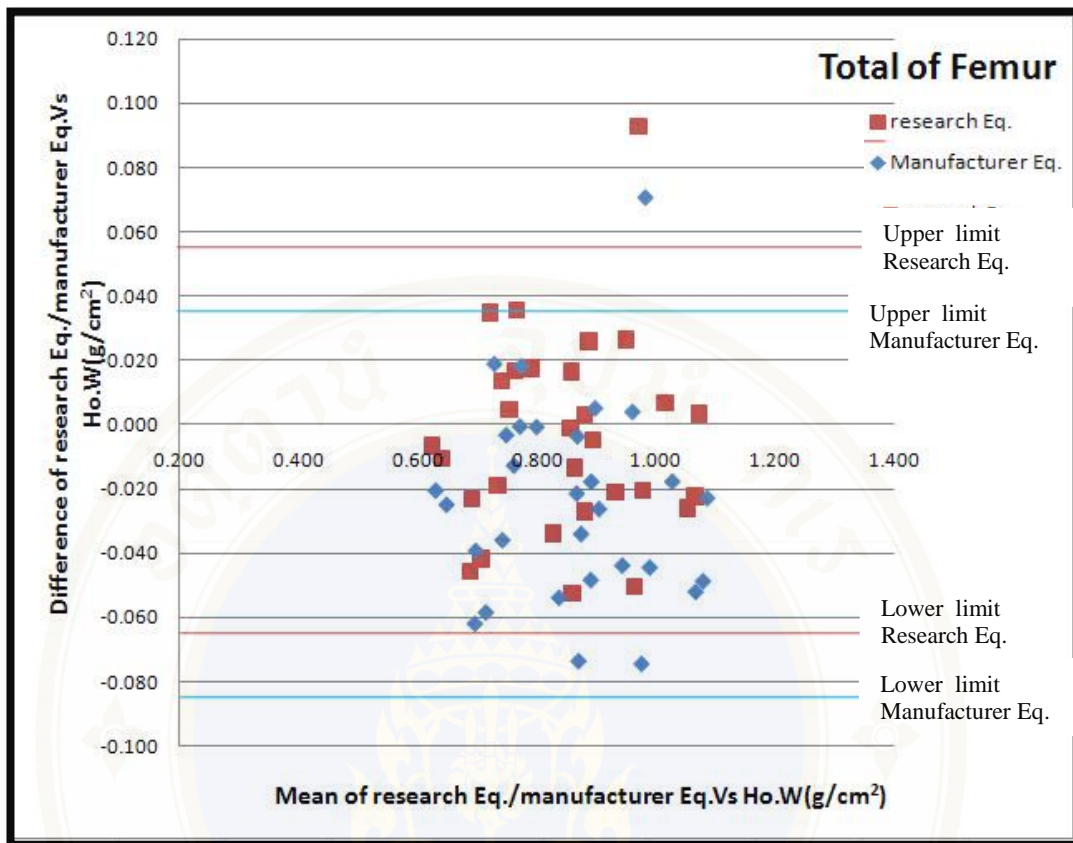


Figure 5.6 Plot of mean and difference Altman and Bland between research’s cross calibration equations vs. manufacturer’s cross calibration equations in Lunar Prodigy and Hologic Discovery W at the total hip

3.3 The comparison between Hologic Discovery A and Hologic Discovery W were shown in table 5.8 The Plot of mean and difference Altman and Bland between research’s cross calibration equations vs. manufacturer’s cross calibration equations in Hologic Discovery A and Hologic Discovery W at the lumbar spine were shown in Figure 5.7 the neck of femur were shown in Figure 5.8 and the total hip were shown in Figure 5.9

Table 5.8 95% confidence interval of difference between observed and predicted BMD using research equations and manufacturer equations (cross calibration equations between Hologic Discovery A and Hologic Discovery W)

	Research Equations	Manufacturer Equations
	95% confidence interval	95% confidence interval
Lumbar spine	-0.0348 - 0.0346	-0.0638 - 0.0056
Neck of femur	-0.0634 - 0.0512	-0.0583 - 0.0563
Total hip	-0.0605 - 0.0557	-0.0474 - 0.0721

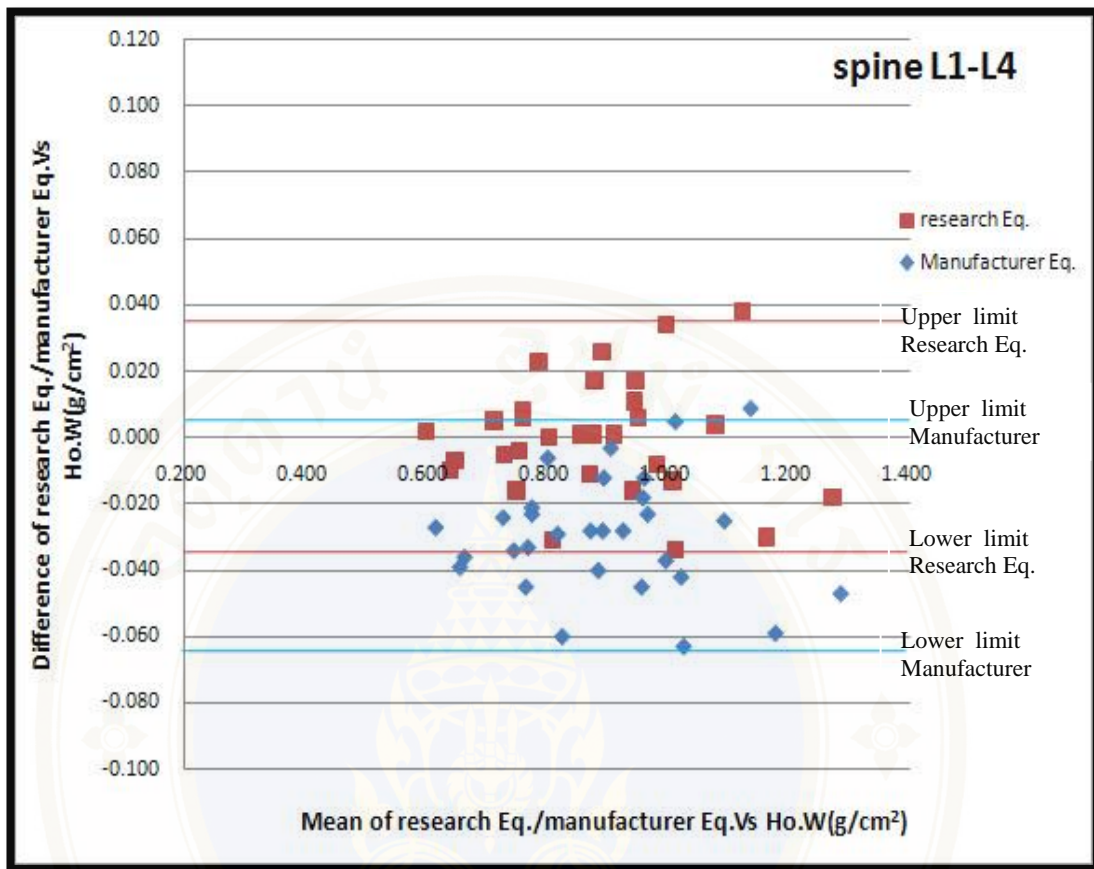


Figure 5.7 Plot of mean and difference Altman and Bland between research’s cross calibration equations vs. manufacturer’s cross calibration equations in Hologic Discovery A and Hologic Discovery W at the lumbar spine

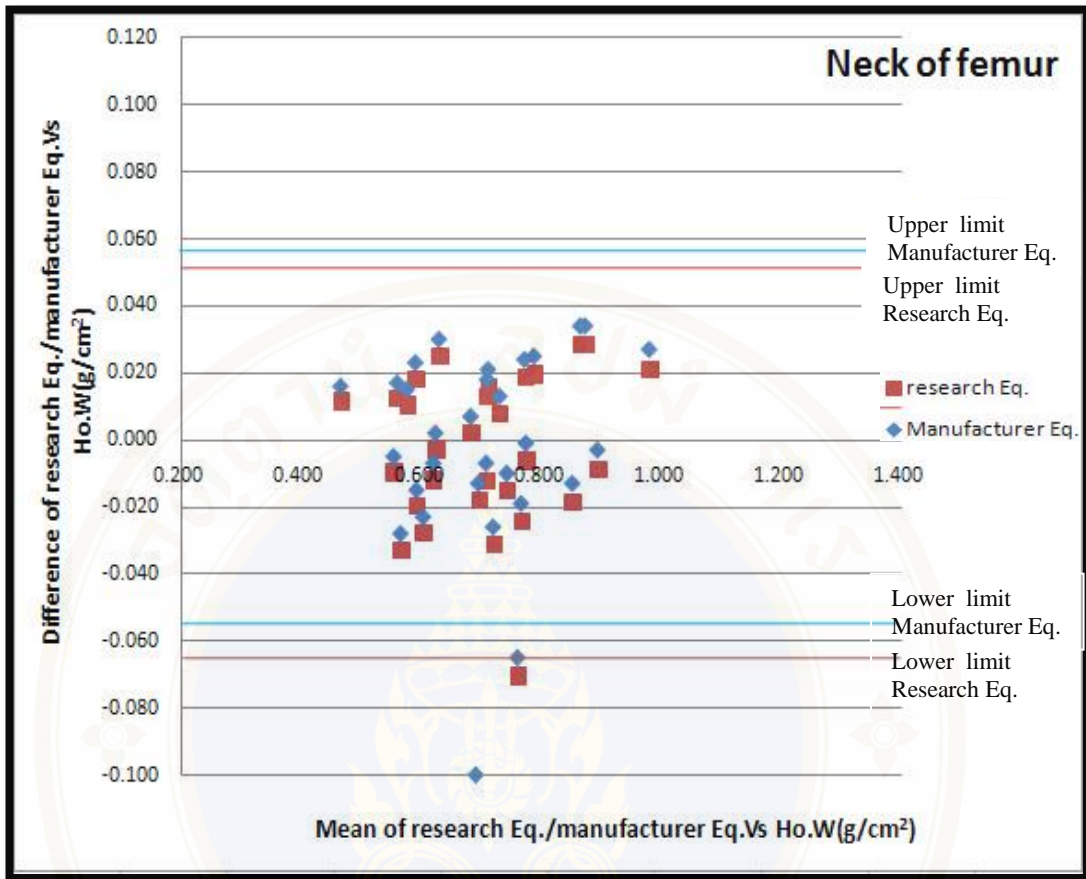


Figure 5.8 Plot of mean and difference Altman and Bland between research’s cross calibration equations vs. manufacturer’s cross calibration equations in Hologic Discovery A and Hologic Discovery W at the neck of femur

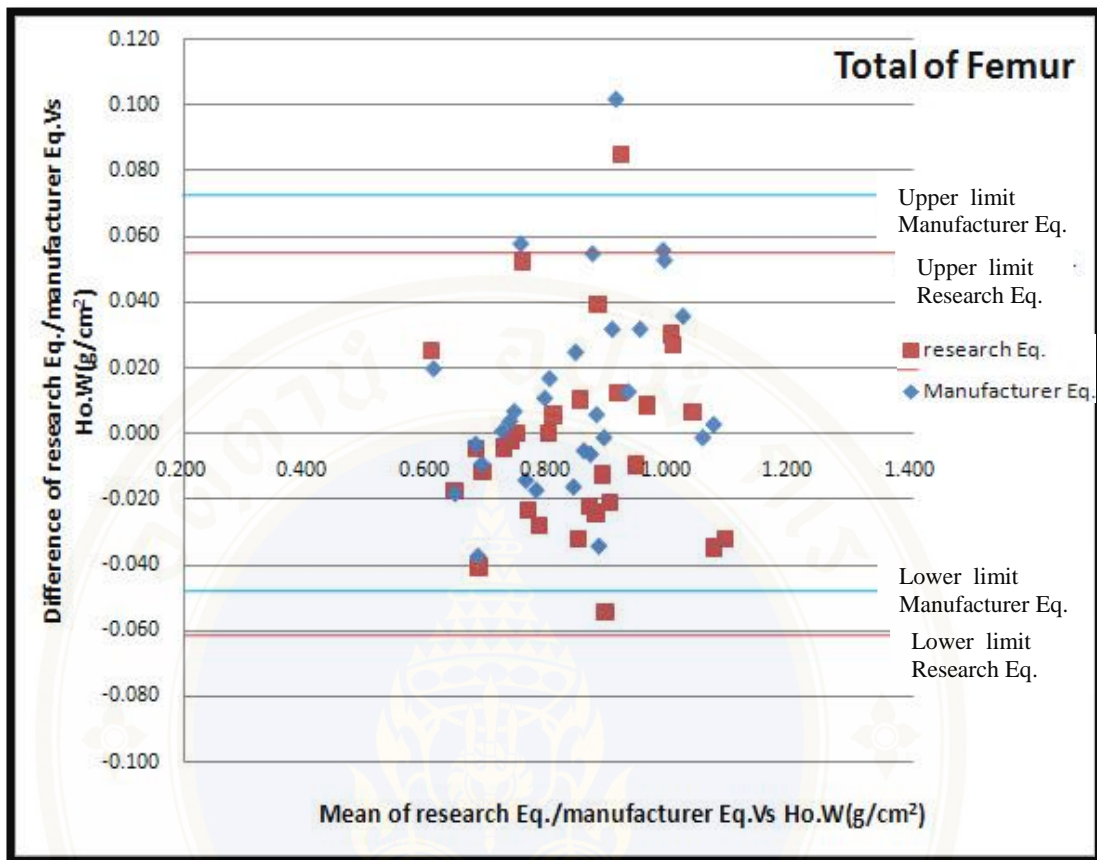


Figure 5.9 Plot of mean and difference Altman and Bland between research’s cross calibration equations vs. manufacturer’s cross calibration equations in Hologic Discovery A and Hologic Discovery W at the total hip

CHAPTER VI

DISCUSSION AND CONCLUSION

6.1 Discussion

Generalized Least Significant Change (GLSC) has clinical applications in monitoring disease progression or treatment effect in bone mineral density (BMD) and bone mineral content. The main purpose of the research was to generate the GLSC values among three DXA machines at division of Nuclear Medicine, Ramathibodi Hospital. The generated GLSC values would help the clinicians monitoring the BMD to make decision in patient management. If the magnitude of the difference between a patient's baseline BMD measured on system 1 and their follow-up BMD measured on system 2 is greater than the GLSC, then there is 95% confidence that a true change in BMD has occurred and if the difference between a patient's baseline BMD measure on system 1 and their follow up BMD measure on system 2 is less than the GLSC, that is less than 95% confidence interval of the precision error, we cannot conclude that the change is genuine.

The next objective was to assess if it was appropriate to use linear regression, cross-calibration equations to predict BMD measurements of one DXA machine from the others. For this, we estimated the difference between the observed (measured) BMDs and the predicted ones. The manufacturer cross-calibration equations were also assessed in the same way.

Bland & Altman plots revealed no linear relationship between the differences and the means of the observed and predicted BMDs using either research or manufacturer cross calibration equations. The differences between the measurements from all 3 pair machines scattered relatively evenly about the x-axis without systematic trend, indicating the lack of association between the precision error and the magnitude of the BMDs. This implies that systematic bias is minimal, if at all present.

The research's cross calibration equations and manufacturer's cross-calibration equations from Lunar Prodigy to Hologic Discovery A were statistically significant at the lumbar spine (p-value 0.027) and total hip (p-value 0.000) but not statistically significant at the neck of femur (p-value 0.483), Lunar Prodigy to Hologic Discovery W were statistically significant at the lumbar spine (p-value 0.000) and total hip (p-value 0.014) but not statistically significant at the neck of femur (p-value is 0.148). Hologic Discovery A to Hologic Discovery W were statistically significant at the lumbar spine (p-value 0.000) but not statistically significant at the neck of femur (p-values 0.501) and total hip (p-values 0.063).

This study followed the International Society for Clinic Densitometry (ISCD) in vivo cross-calibration protocol. All densitometers were calibrated daily and weekly for quality control in the morning before their use so all measurements were deemed to be accurate. One technologist positioned and analyzed volunteers on all machines, to avoid inter-observer variation. Repeated measurements were performed for all machines, the average measurement for each site may have made for more accurate measurement at each site, and the cross calibration for all DXA systems may have been more accurate. Repositioning volunteers were performed when repeated measurement for all DXA systems may have made close to actual measurement in the patients between baseline and follow up measurement.

Ideally, a patient should be followed-up with the DXA system used at baseline. However, often this is impractical. In general, the manufacturers provide a conversion equation, typically a linear regression, to estimate the BMD values from or to their DXA machine. Nevertheless, the ISCD recommends that the manufacturer's conversion equation should not be used at individual DXA centers. Little is known regarding how manufacturers performed testing. It generally is believed that manufacturers use young normal subjects with no degenerative changes and that expert technologists perform the scans. Furthermore, it is not known how many subjects are used or how many repeat scans are conducted. Overall, the manufacturers may not reflect position data that are commonly encountered in the clinic. The DXA centers should determine and use their own GLSC when comparing measurements performed on 2 different systems. Our attempt to generate conversion or predictive equations from one system to another resulted in relatively large differences between

the observed and predicted BMDs. Therefore, the prediction method should only be used when there is no alternative. The differences between our equations and the manufactures' were of similar range. However, the latter tend to span over negative values, particularly at the lumbar spine and, more so, the total hip, suggesting systematic bias toward overestimation.

6.2 Conclusion

The GLSCs between Lunar Prodigy, Hologic Discovery A and Hologic Discovery W have been estimated. These GLSCs should be used when comparing the BMDs measured from different DXA machines. The cross – calibration equations have also been derived but the prediction errors are larger than the GLSCs. Hence, the GLSCs should be used when comparing the BMDs from different DXA machines.

REFERENCES

1. Fogelman I, Blake GM. Different approaches to bone densitometry. *J Nucl Med.* 2000 Dec;41(12):2015-25.
2. Taechakraichana N AP, Panyakhamlerd K, Limpaphayom K. . Postmenopausal osteoporosis: what is the real magnitude of the problem in the Thai population. *J Med Assoc Thai.* 1998;81:397-401.
3. Limpaphayom K. Health Aging in the 21st century The 6th international menopause society world congress on the menopause. 1999.
4. Hammami M, Picaud J-C, Fusch C, Hockman EM, Rigo J, Koo WWK. Phantoms for Cross-Calibration of Dual Energy X-ray Absorptiometry Measurements in Infants. *J Am Coll Nutr* 2002;21(4):328-32.
5. ISCD. International Society for Bone Densitometry Technologist Course Syllabus and Associated reading Materials 8ed2008.
6. Johnson DR. Introductory Anatomy: Bones. 2005; Available from: <http://www.leeds.ac.uk/chb/lectures/anatomy3.html>.
7. Buckwalter JA. Principles and their application Turek's Orthopedics. 6 ed. Philadelphia: Lippincott Williams & Wilkins; 2005. p. 3-56.
8. Shier D, Butter J, Lewis R. Hole's Human Anatomy Physiology 1996.
9. WHO Scientific group. Prevention and Management of Osteoporosis. Geneva 2003.
10. Lewiecki EM, Baim S, Binkley N, Bilezikian JP, Kendler DL, Hans DB, et al. Report of the International Society for Clinical Densitometry 2007 Adult Position Development Conference and Official Positions. *Southern Medical Journal.* 2008;101(7):735-910.
11. Royal Adelaide Hospital. 2009; Available from: http://www.rah.sa.gov.au/nucmed/BMD/bmd_equipment.htm.
12. Nelson B. Watts. Fundamentals and pitfalls of bone densitometry using dual-energy X-ray absorptiometry (DXA) *Osteoporosis International.* 2004;15(11):847-54

13. ISCD. About ISCD. 2009; Available from:
<http://www.iscd.org/visitors/about/AboutISCD.cfm>.
14. Shepherd JA, Lu Y, Wilson K, Fuerst T, Genant H, Hangartner TN, et al. Cross-calibration and minimum precision standards for dual-energy X-ray absorptiometry: the 2005 ISCD Official Positions. *J Clin Densitom.* 2006 Jan-Mar;9(1):31-6.
15. Shepherd JA, Lu Y. A generalized least significant change for individuals measured on different DXA systems. *J Clin Densitom.* 2007 Jul-Sep;10(3):249-58.
16. GraphPad Software. 2005; Available from:
<http://www.graphpad.com/quickcalcs/random2.cfm>.
17. Bland JM, Altman DG. Applying the right statistics: analyses of measurement studies. *Ultrasound Obstet Gynecol* 2003;22: 85-9.



APPENDIX A

Definitions

Absorptiometry – A method for measuring bone mineral density using the attenuation of x or gamma radiation

Age-matched – A comparison of the patient's BMD to a reference population of subjects the same age and gender as the patient

Bisphosphonates – A group of drugs that are similar to a naturally occurring compound called pyrophosphate that is found in bone

Bone density – The ratio of bone mass to volume, indicating bone compactness. Bone density increases rapidly through adolescence, more slowly until about age 35, and then plateaus and declines. Bone density is measured most frequently in the spine, hip, wrist, forearm, and/or heel for the detection and diagnosis of osteoporosis

Bone formation – That part of the bone-remodeling cycle in which osteoblasts synthesize a protein matrix of fibers upon which crystals of calcium and phosphorus are embedded during mineralization to provide strength and rigidity

Bone mass – The amount of mineral in a bone. Although this is different from the bone density, the terms are often used interchangeably

Bone mineral content (BMC) – The total quantity of material (bone mineral) measured by absorptiometry. Bone mineral content is measured in grams; the quantity is often used to follow change over time in a single subject

Bone mineral density (BMD) – The quantity calculated by dividing the measured bone mineral content by the measured bone area in a densitometry study. The bone mineral density carries units of gram per square centimeter and is most often compared to reference population values

Bone remodeling – The cyclic process of bone breakdown and formation that is responsible for growth, maintenance, and repair for bone tissue

Bone remodeling unit (BMU) – A group of cells (osteoclasts and osteoblasts) that create one new packet of bone. In normal trabecular bone approximately 900 BMU

are activated each day, while in cortical bone approximately 180 BMU will be activated daily

Bone resorption – The breakdown part of bone's life cycle, during which the old and damaged bone tissue is resorbed. Osteoporosis occurs when resorption is greater than formation

Coefficient of Variation (%CV) – A value often used to reflect precision. The coefficient of variation which can be presented in absolute or percentage terms is often preferred to the standard deviation because it adjusts for measurement size by dividing the standard deviation by the mean.

Cortical bone – Dense, hard bone with microscopic spaces. Cortical bone is typically found in long bones such as the femur, forearm, and tibia. Eighty percent of the skeleton is made up of cortical bone.

Densitometer – An instrument that measures the density of bones by determining the amount of radiation that the bones absorb

Dual energy x-ray absorptiometry (DXA) – A type of bone-density testing that uses 2 energy x-ray to measure bone density.

Generalized Least significant change (GLSC) – is used to compare two scans from a patient when measured on two different DXA systems.

Hydroxyapatite – An inorganic compound found in the matrix of bone and the teeth, which gives rigidity to these structures. Its chemical formula, hydroxyapatite is $\text{Ca}_{10}(\text{PO}_4)_6(\text{OH})_2$

Least significant change (LSC) – The amount of change in bone density needed to be statistically confident that a real change has occurred.

Lumbar spine – The five individual bones or vertebrae in the lower back

Osteoblasts – Small cells that fill in the cavities dug by the osteoclasts and produce the collagen matrix of new bone

Osteoclasts – Large cells that initiate the bone remodeling cycle by digging cavities in the existing bone tissue

Osteocytes – mature osteoblasts embedded in newly-mineralized bone

Osteopenia – This term refers to a decrease in bone mineral density that, although too low to be called normal, is not low enough to be considered osteoporotic

Osteoporosis – A systemic skeletal disease characterized by low bone mass and microarchitectural deterioration of bone tissues, leading to enhanced fragility and increased fracture risk.

Peak bone mass – A concept that bone mass has a maximal level given optimal conditions. Peak bone mass is believed to be controlled by genetic factors (age, gender, and body size) and significantly impacted by environmental factors (nutrition, exercise, and general health). The concept of peak bone mass is important to the study of bone disease in that if an individual achieves maximal (peak) bone mass, they may reduce the risk of serious bone loss

Prevalence – The frequency of disease at a specific point in time (number with disease/risk); often expressed as number per 1,000 people

Quality Assurance (QA) – A series of tests that calibrate the system, monitor its ability to meet performance specifications and acquire daily standard values which are used in the calibration of scan results

Region of interest (ROI) – The anatomical area that is scanned and analyzed for which BMD values are calculated; the skeletal site or defined area that is being measured

Resorption – The stage of bone breakdown in the bone remodeling process; resorption is carried out by the osteoclast

Standard deviation (SD) – Estimates the variability of the sample values from the sample mean

Trabecular bone – The porous, spongy bone that lines the bone marrow cavity and is surrounded by cortical bone. Trabecular bone makes up 20% of the skeletal mass (80% of the surface area)

T-score – A value in bone density used primarily for the diagnosis of osteoporosis. It is a patient's measure of the number of standard deviations from the mean at which peak bone density is achieved

WHO criteria – World Health Organization diagnostic categories of normal, osteopenia, osteoporosis, and severe osteoporosis. These are based on the number of standard deviations above or below the young adult mean that the patient's BMD value lies

Z-score – The Z-score is a measure of deviation from the reference population expressed in units of the population’s standard deviation. The Age Matched Z-score indicates how much the patient deviates from the mean Age Matched values



APPENDIX B**Consent Form**

ชื่อโครงการวิจัย การศึกษาเปรียบเทียบค่าความหนาแน่นของกระดูกระหว่างเครื่องวัดความหนาแน่นของกระดูกโดยการใช้เอกซเรย์ 2 ค่าพลังงาน 3 เครื่อง (เครื่อง Hologic รุ่น Discovery A, รุ่น Discovery W และ เครื่อง Lunar รุ่น Prodigy)

ชื่อผู้วิจัย _____

ชื่อผู้เข้าร่วมการวิจัย _____

อายุ _____ ปี เลขที่เวชระเบียน _____

คำยินยอมของผู้เข้าร่วมการวิจัย

ข้าพเจ้า นาย/นาง/นางสาว _____ ได้รับทราบรายละเอียดของโครงการวิจัยตลอดจนประโยชน์ และผลข้างเคียงอันอาจเกิดต่อตัวข้าพเจ้าจากผู้วิจัยแล้วอย่างชัดเจน ไม่มีสิ่งใดปิดบังซ่อนเร้นและยินยอมให้ทำการวิจัยในโครงการที่มีชื่อข้างต้น และข้าพเจ้ารู้ว่าถ้ามีปัญหาหรือข้อสงสัยเกิดขึ้น ข้าพเจ้าสามารถสอบถามผู้วิจัยได้

ข้าพเจ้าสามารถไม่เข้าร่วมโครงการวิจัยนี้เมื่อใดก็ได้โดยไม่มีผลกระทบต่อการใช้บริการหรือการรักษาที่ข้าพเจ้าจะได้รับ

นอกจากนี้ผู้วิจัยจะเก็บข้อมูลเกี่ยวกับข้าพเจ้าเป็นความลับ และจะเปิดเผยได้เฉพาะในรูปแบบที่เป็นสรุปผลการวิจัย การเปิดเผยข้อมูลเกี่ยวกับข้าพเจ้าต่อหน่วยงานต่างๆที่เกี่ยวข้องจะกระทำเฉพาะกรณีจำเป็น ด้วยเหตุผลทางวิชาการ

ลงนาม.....ผู้เข้าร่วมการวิจัย

()

วันที่...../...../.....

คำอธิบายของแพทย์

ข้าพเจ้าได้อธิบายรายละเอียดของโครงการตลอดจนประโยชน์ของการวิจัย รวมทั้งข้อเสีย
ที่อาจเกิดขึ้นแก่ผู้เข้าร่วมการวิจัยทราบดีแล้วอย่างชัดเจน โดยไม่มีสิ่งใดปิดบังซ่อนเร้น

ลงนาม.....แพทย์ผู้วิจัย

()

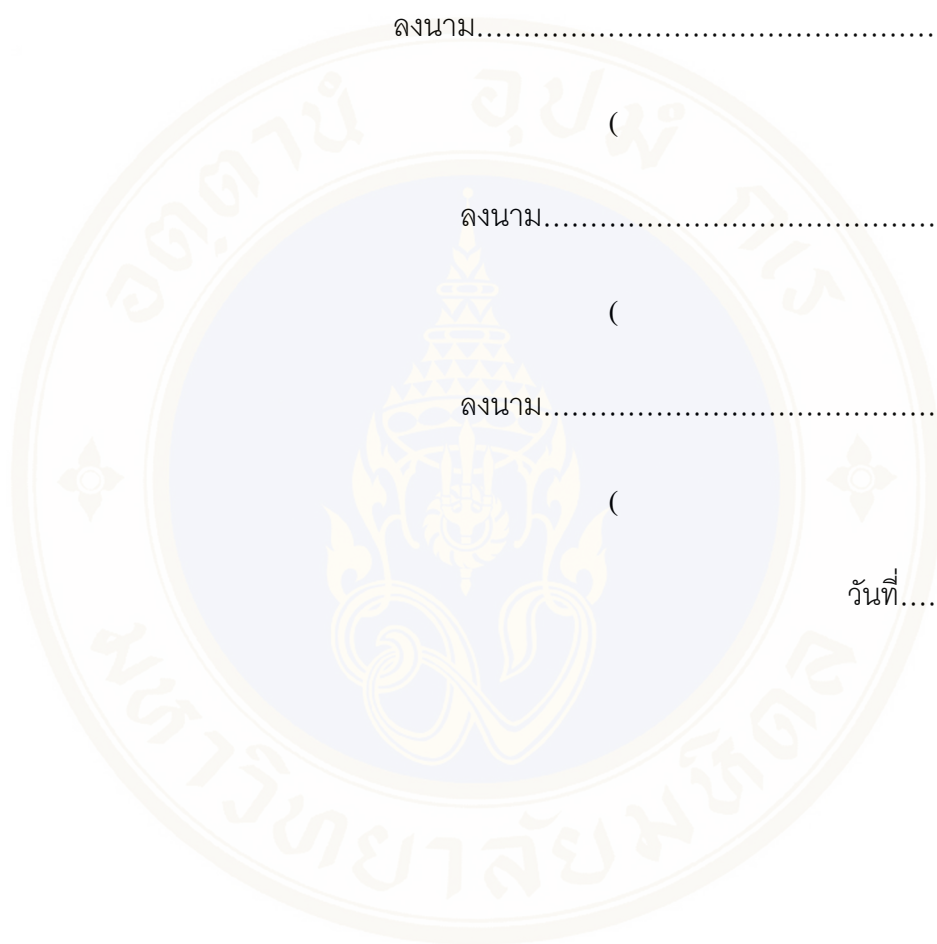
ลงนาม.....พยาน

()

ลงนาม.....พยาน

()

วันที่...../...../.....



APPENDIX C

Patient Information Sheet

ชื่อโครงการวิจัย การศึกษาเปรียบเทียบค่าความหนาแน่นของกระดูกระหว่างเครื่องวัดความหนาแน่นของกระดูกโดยการใช้เอกซเรย์ 2 ค่าพลังงาน 3 เครื่อง (เครื่อง Hologic รุ่น Discovery A, รุ่น Discovery W และ เครื่อง Lunar รุ่น Prodigy)

สถานที่ทำการวิจัย หน่วยเวชศาสตร์นิวเคลียร์ ภาควิชารังสีวิทยา

ผู้ทำการวิจัย ผู้ช่วยศาสตราจารย์แพทย์หญิงชนิกา ศรีธรา

บุคคลและวิธีการติดต่อเมื่อมีเหตุฉุกเฉินหรือความผิดปกติที่เกี่ยวข้องกับการวิจัย

ผู้ช่วยศาสตราจารย์แพทย์หญิงชนิกา ศรีธรา โทรศัพท์ 02 021 1192

ความเป็นมาของโครงการ

เนื่องจากค่า BMD เป็นค่าที่มีความสำคัญในการประเมินภาวะและการติดตามผลการรักษาของผู้ป่วยโรคกระดูกพรุน ดังนั้นความถูกต้องและความแม่นยำในการหาค่า BMD จึงมีความสำคัญอย่างมาก โดยเฉพาะอย่างยิ่งในการรักษาโรคกระดูกพรุน จะต้องทำการตรวจปีละ 1 ครั้งซึ่งค่า BMD ที่ได้ในแต่ละครั้งจะต้องนำมาเปรียบเทียบกับค่า BMD ที่ได้ในครั้งแรก หรือ ก่อนหน้า เพื่อจะบอกประสิทธิภาพของการรักษา ทำให้ต้องควบคุมปัจจัยต่างๆในการตรวจหาค่า BMD ให้ใกล้เคียงกับครั้งแรก หรือ ก่อนหน้า ซึ่งเครื่องแต่ละยี่ห้อและแต่ละรุ่นจะใช้เทคนิคในการตรวจวัดต่างกัน โดยเครื่องแต่ละยี่ห้อก็จะแตกต่างกันที่การผลิตเพื่อให้ได้ x-ray 2 ค่าพลังงาน และในเครื่องแต่ละรุ่นก็จะต่างกันที่หัววัดรังสี ซึ่งทั้ง 2 ปัจจัยนี้มีผลกับการคำนวณค่าทาง quantitative ดังนั้น เมื่อทางหน่วยงานมีการเปลี่ยนเครื่องตรวจหาความหนาแน่นของกระดูกเช่น เปลี่ยนยี่ห้อ หรือเปลี่ยนรุ่น จึงมีผลกับการเปรียบเทียบค่า BMD ระหว่างเครื่องในครั้งก่อนหน้า และเครื่องในครั้งปัจจุบัน จึงเป็นที่มาของการศึกษาวิจัยนี้

การทำ cross-calibration เป็นการปรับเทียบเครื่องมือเพื่อให้สามารถทำการเปรียบเทียบค่า BMD ระหว่างเครื่อง DXA 3 เครื่อง คือ เครื่อง HOLOGIC รุ่น Discovery A กับ เครื่อง HOLOGIC รุ่น Discovery W และ เครื่อง LUNAR รุ่น Prodigy

วัตถุประสงค์

เพื่อศึกษา Least Significant change (LSC) และ ทำนายความสัมพันธ์ของค่า BMD จากเครื่องใดเครื่องหนึ่งจากทั้ง 3 เครื่อง ที่ได้จากการตรวจหาความหนาแน่นของกระดูกด้วยเครื่อง DXA (Dual Energy X-ray Absorptiometry) ระหว่างเครื่อง HOLOGIC Discovery A กับ เครื่อง HOLOGIC Discovery W และ เครื่อง Prodigy LUNAR

รายละเอียดที่จะปฏิบัติต่อผู้เข้าร่วมการวิจัย

อาสาสมัครจะได้รับฟังคำชี้แจงและซักถามเกี่ยวกับโครงการ ต่อเมื่ออาสาสมัครเข้าใจและลงนามในใบยินยอมจึงจะทำการเก็บข้อมูลจากอาสาสมัคร

จากนั้นจะทำการวัดความหนาแน่นของกระดูกโดยและทำการตรวจหาค่า BMD ส่วน spine และ femur โดยทำการตรวจห่างกันไม่เกิน 60 วัน จากนั้น บันทึกข้อมูลค่า BMD ที่ได้จากทั้ง 3 เครื่องและนำข้อมูลที่ได้มาวิเคราะห์หาค่าความหนาแน่น ค่า least significant change (LSC) และ ค่าความสัมพันธ์ของค่า BMD จากเครื่องใดเครื่องหนึ่งจากทั้ง 3 เครื่อง ตามมาตรฐานสากลของ ISCD

ประโยชน์ต่ออาสาสมัคร

ผู้เข้าร่วมการวิจัยจะได้รับการตรวจวัดความหนาแน่นและการติดตามการรักษาโรคกระดูกพรุนได้อย่างถูกต้องได้มาตรฐาน

ความไม่สะดวกหรือผลข้างเคียงที่เกิดจากการวิจัย

ไม่มีผลข้างเคียง อาสาสมัครจะได้รับปริมาณรังสีเล็กน้อยเทียบเท่ากับการถ่ายภาพรังสีที่กระดูกสันหลัง และเสียเวลาเพิ่มขึ้นประมาณสามสิบนาที

การเก็บข้อมูลเป็นความลับ

ข้อมูลที่ได้จะถูกเก็บเป็นความลับและจะใช้เฉพาะในทางวิชาการและการพัฒนาคุณภาพงานเท่านั้น

APPENDIX D

Questionnaire

ชื่อ - สกุล		HN	
วัน/เดือน/ปี เกิด		อายุ	
หน้าหนัก		ส่วนสูง	
ปัจจัยเสี่ยง	มี	ไม่มี	หมายเหตุ
1. กระจกหัก			บริเวณ
2. สูบบุหรี่			สูดดม ครั้ง/สัปดาห์ ไม่สูดดม ครั้ง/สัปดาห์
3. ดื่มแอลกอฮอล์			สูดดม ครั้ง/สัปดาห์ ไม่สูดดม ครั้ง/สัปดาห์
4. การออกกำลังกาย			สูดดม ครั้ง/สัปดาห์ ไม่สูดดม ครั้ง/สัปดาห์
5. ดื่มนม			สูดดม ครั้ง/สัปดาห์ ไม่สูดดม ครั้ง/สัปดาห์
6. ยาที่รับประทานเป็นประจำ			ชื่อยา
			ชื่อยา
			ชื่อยา
			ชื่อยา
7. โรคประจำตัว			โรค
			โรค
			โรค
8. บิดามารดา เคยมีกระดูกสันหลังหัก			
9. เคยแพ้ดื้ออินซูลิน หรือรังไข่, เป็นโรคขาดสารอาหาร, ให้เคมีบำบัดในมะเร็งเต้านม			
10. มีปัญหาเกี่ยวกับระบบลำไส้ เช่น Chom's disease			
11. ไม่มีการเคลื่อนไหวตามปกติเป็นระยะเวลาาน เช่น มีปัญหากล้ามเนื้อสปีด, Parkinson's disease			
12. มีการผ่าตัดเปลี่ยนอวัยวะ			
13. เป็นโรคเบาหวาน ในขั้นที่1			
14. เป็นโรคเกี่ยวกับต่อมธัยรอยด์ เช่น Hypertthyroid ที่ยังไม่ได้รับการรักษา			
15. หมดประจำเดือนก่อน อายุ 45ปี			
16. มีภาวะโรคตับเรื้อรัง			

BIOGRAPHY

NAME	Miss. Sasithorn Amnuaywattakorn
DATE OF BIRTH	26 July 1977
PLACE OF BIRTH	Bangkok, Thailand
INSTITUTIONS ATTENDED	Mahidol University, 2000 Bachelor of Science (Radiological Technology)
	Mahidol University, 2011 Master of Science (Medical Physics)
HOME ADDRESS	204 Prachachuen Road, Bangzue, Bangzue Bangkok, Thailand 10800